

NON-MINIMAL HIGGS INFLATION AND NON-THERMAL LEPTOGENESIS IN A SUPERSYMMETRIC PATI-SALAM MODEL

C. PALLIS AND N. TOUMBAS

*Department of Physics, University of Cyprus,
P.O. Box 20537, CY-1678 Nicosia, CYPRUS*

ABSTRACT

We consider a supersymmetric (SUSY) Grand Unified Theory (GUT) based on the gauge group $G_{\text{PS}} = SU(4)_C \times SU(2)_L \times SU(2)_R$, which incorporates non-minimal chaotic inflation, driven by a quartic potential associated with the Higgs fields involved in the spontaneous breaking of G_{PS} . The inflationary model relies on renormalizable superpotential terms and does not lead to overproduction of magnetic monopoles. It is largely independent of the one-loop radiative corrections and can become consistent with the current observational data on the inflationary observables, with the symmetry breaking scale of G_{PS} assuming its SUSY value. Within our model, the strong CP and the μ problems of the minimal SUSY standard model can be resolved via a Peccei-Quinn symmetry. Moreover baryogenesis occurs via non-thermal leptogenesis realized by the out-of-equilibrium decay of the right-handed neutrinos, which are produced by the inflaton's decay. We consider two versions of such a scenario, assuming that the inflaton can decay to the lightest or to the next-to-lightest right-handed neutrino. Both scenarios can become compatible with the constraints arising from the baryon asymmetry of the universe, the gravitino limit on the reheating temperature and the upper bound on the light neutrino masses, provided that the gravitino is somehow heavy. In the second scenario, extra restrictions from the $SU(4)_C$ GUT symmetry on the heaviest Dirac neutrino mass and the data on the atmospheric neutrino oscillations can be also met.

KEYWORDS: Cosmology, Supersymmetric models;
PACS CODES: 98.80.Cq, 12.60.Jv

CONTENTS

1	INTRODUCTION	1
2	THE PATI-SALAM SUSY GUT MODEL	2
3	THE INFLATIONARY SCENARIO	7
3.1	STRUCTURE OF THE INFLATIONARY ACTION	7
3.2	THE INFLATIONARY OBSERVABLES – REQUIREMENTS	11
3.3	NUMERICAL RESULTS	13
4	NON-THERMAL LEPTOGENESIS	14
4.1	THE GENERAL SET-UP	15
4.2	IMPOSED CONSTRAINTS	19
4.3	NUMERICAL RESULTS	20
5	CONCLUSIONS	22
	APPENDIX A: DERIVATION OF THE MASS SPECTRUM DURING NON-MHI	23
	APPENDIX B: INFLATON OSCILLATIONS AFTER NON-MHI	26
	REFERENCES	28

1 INTRODUCTION

Non-minimal Higgs inflation (non-MHI) [1–3] – see also Ref. [4] – is an inflationary model of chaotic type which arises in the presence of a non-minimal coupling between a Higgs-inflaton field and the Ricci scalar curvature, \mathcal{R} . It has been shown that non-MHI based on a quartic potential with a quadratic non-minimal coupling to gravity can be realized in both a non-supersymmetric [1] and a *supersymmetric* (SUSY) framework [3], provided that the coupling of the inflaton to \mathcal{R} is strong enough. In most of the existing models, the inflaton is identified with the Higgs field(s) of the *Standard Model* (SM) or the next-to-MSSM (*Minimal SUSY SM*) [3] – for non-minimal inflation driven by an inflaton other than the Higgs field see Ref. [5–9] for non-SUSY models and Ref. [10–12] for SUSY ones.

On the other hand, SUSY GUTs arise as natural extensions of Physics beyond the MSSM. Within their framework, a number of challenges – such as the μ problem, the generation of the observed *baryon asymmetry of the universe* (BAU) and the existence of tiny but non-zero neutrino masses – which the MSSM fails to address can be beautifully arranged. The achievement of gauge coupling unification within the MSSM suggests that the breaking of the GUT gauge symmetry group down to the SM one, $G_{\text{SM}} = SU(3)_C \times SU(2)_L \times U(1)_Y$, occurs at a scale $M_{\text{GUT}} \simeq 2 \cdot 10^{16}$ GeV through some Higgs superfields. Therefore, the latter arise naturally as candidates for driving non-MHI – for earlier attempts within non-SUSY $SU(5)$ GUT see Ref. [13]. In a such situation the GUT gauge group is already spontaneously broken during non-MHI through the non-zero values acquired by the relevant Higgs fields. Consequently, non-MHI does not lead to the production of topological defects. Moreover, the potential of non-MHI possesses a non-zero classical inclination and so, the inflationary dynamics is largely independent of the radiative corrections. As a consequence, the *vacuum expectation values* (v.e.vs) which the Higgs fields acquire at the end of non-MHI can be exactly equal to the values required by the unification of the MSSM gauge couplings. Finally, the predicted inflationary observables are consistent with the fitting [14] of the seven-year data of the *Wilkinson Microwave Anisotropy Probe Satellite* (WMAP7), *baryon-acoustic-oscillations* (BAO) and *Hubble constant* (H_0) data.

These features are to be contrasted with the widely adopted models of standard SUSY *hybrid inflation* (HI) [15], where the spontaneous breaking of the GUT gauge symmetry takes place at the end

of HI and, thus, topological defects are copiously formed [16] if they are predicted by the symmetry breaking. This is because, the standard SUSY HI is typically driven by a singlet field whereas the Higgs fields are confined to zero where the GUT symmetry is unbroken. Avoidance of cosmologically disastrous topological defects can be obtained within smooth [16, 17] or shifted [18, 19] HI by using either non-renormalizable [16, 19] or renormalizable [17, 18] superpotential terms, which generate stable inflationary trajectories with non-zero values for the Higgs fields. Some of the latter constructions, though, are much more complicated than the simplest original model [15]. In the cases of standard [15] and shifted [18, 19] HI, radiative corrections play an important role in creating the slope of the inflationary potential and the v.e.vs of the Higgs fields turn out to be mostly lower than the GUT SUSY symmetry scale, since the relevant mass scale is constrained by the normalization of the curvature perturbation [14]. Finally, all types of HI suffer from the problem of an enhanced (scalar) spectral index, n_s , which turns out to be, mostly, well above the current data [14]. For several proposals aiming to improve on the latter shortcoming of SUSY HI see Ref. [20–24].

In this paper we present a model of non-MHI, adopting a SUSY GUT model based on the *Pati-Salam* (PS) gauge group $G_{\text{PS}} = SU(4)_C \times SU(2)_L \times SU(2)_R$. Note that SUSY PS GUT models are motivated [25] from recent D-brane constructions and can also arise [26] from the standard weakly coupled heterotic string. Employing only renormalizable superpotential terms, we then show that the model naturally leads to non-MHI within SUGRA avoiding thereby the overproduction of unwanted monopoles. Also the inflationary observables turn out to lie within the current data [14]. Our model possesses a number of other interesting features too. The μ -problem of the MSSM can be solved [27] via a Peccei-Quinn (PQ) symmetry, which also solves the strong CP problem, and the proton is practically stable. Light neutrinos acquire masses by the seesaw mechanism [29] and the BAU can be generated through primordial non-thermal [30] leptogenesis. We single out two cases according to whether the inflaton decays to the lightest [31] or the next-to-lightest [32] *right-handed* (RH) neutrino. In both cases the constraints arising from the gravitino (\tilde{G}) limit [33–35] on the reheating temperature and the BAU can be met provided that the masses of \tilde{G} lie in the multi-TeV region. On the other hand, the second scenario gives us the opportunity to combine the calculation of BAU with the present neutrino data [36] and the prediction of G_{PS} for the masses of the fermions of the third generation.

The plan of this paper is as follows. We present the basic ingredients – particle content and structure of the superpotential and the Kähler potential– of our model in Sec. 2. In Sec. 3 we describe the inflationary potential, derive the inflationary observables and confront them with observations. In Sec. 4 we outline the two scenaria of non-thermal leptogenesis, exhibit the relevant imposed constraints and restrict the parameters of our model for each scenario. Our conclusions are summarized in Sec. 5. Details concerning the derivation of the mass spectrum of the theory during non-MHI are arranged in Appendix A whereas effects of instant preheating potentially important for some values of the parameters are discussed in Appendix B. Throughout the text, we use natural units for Planck’s and Boltzmann’s constants and the speed of light ($\hbar = c = k_B = 1$); the subscript of type χ denotes derivation *with respect to* (w.r.t) the field χ (e.g., ${}_{,\chi\chi} = \partial^2/\partial\chi^2$); charge conjugation is denoted by a star and $\log [\ln]$ stands for logarithm with basis 10 [e].

2 THE PATI-SALAM SUSY GUT MODEL

We focus on a SUSY PS GUT model described in detail in Ref. [19] – see also Ref. [37]. The representations and the transformation properties of the various superfields contained in the model under G_{PS} , their decomposition under G_{SM} , as well as their extra global charges are presented in Table 1. Recall that, in the PS GUT models, the SM hypercharge Q_Y is identified as the linear combination $Q_Y = Q_{T_R^3} + Q_{(B-L)}/2$ where $Q_{T_R^3}$ is the $SU(2)_R$ charge generated by $T_R^3 = \text{diag}(1, -1)/2$ and the $Q_{(B-L)}$ is the $SU(4)_C$ charge generated by $T_C^{15} = \text{diag}(1, 1, 1, -3)/2\sqrt{6}$. Here T_R^m with $m = 1, 2, 3$

are the 3 generators of $SU(2)_R$ and T_C^a with $a = 1, \dots, 15$ are the 15 generators of $SU(4)_C$ with normalizations $\text{Tr}(T_C^a T_C^b) = \delta^{ab}/2$ and $\text{Tr}(T_R^m T_R^k) = \delta^{mk}/2$, where Tr denotes trace of a matrix.

The i th generation ($i = 1, 2, 3$) *left-handed* (LH) quark [lepton] superfields, u_{ia} and d_{ia} – where $a = 1, 2, 3$ is a color index – [e_i and ν_i] are accommodated in a superfield F_i . The LH antiquark [antilepton] superfields u_{ia}^c and d_{ia}^c [e_i^c and ν_i^c] are arranged in another superfield F_i^c . These can be represented as

$$F_i = \begin{pmatrix} q_{i1} & q_{i2} & q_{i3} & l_i \end{pmatrix} \quad \text{and} \quad F_i^c = \begin{pmatrix} q_{i1}^c \\ q_{i2}^c \\ q_{i3}^c \\ l_i^c \end{pmatrix} \quad \text{with}$$

$$q_{ia} = \begin{pmatrix} d_{ia} & -u_{ia} \end{pmatrix}, \quad l_i = \begin{pmatrix} e_i & -\nu_i \end{pmatrix}, \quad q_{ia}^c = \begin{pmatrix} -u_{ia}^c \\ d_{ia}^c \end{pmatrix} \quad \text{and} \quad l_i^c = \begin{pmatrix} -\nu_i^c \\ e_i^c \end{pmatrix}. \quad (2.1)$$

The gauge symmetry G_{PS} can be spontaneously broken down to G_{SM} through the v.e.vs which the superfields

$$H^c = \begin{pmatrix} q_{H1}^c \\ q_{H2}^c \\ q_{H3}^c \\ l_H^c \end{pmatrix} \quad \text{and} \quad \bar{H}^c = \begin{pmatrix} \bar{q}_{H1}^c & \bar{q}_{H2}^c & \bar{q}_{H3}^c & \bar{l}_H^c \end{pmatrix} \quad \text{with}$$

$$q_{Ha}^c = \begin{pmatrix} u_{Ha}^c \\ d_{Ha}^c \end{pmatrix}, \quad l_H^c = \begin{pmatrix} \nu_H^c \\ e_H^c \end{pmatrix}, \quad \bar{q}_{Ha}^c = \begin{pmatrix} \bar{u}_{Ha}^c & \bar{d}_{Ha}^c \end{pmatrix} \quad \text{and} \quad \bar{l}_H^c = \begin{pmatrix} \bar{\nu}_H^c & \bar{e}_H^c \end{pmatrix}, \quad (2.2)$$

acquire in the directions ν_H^c and $\bar{\nu}_H^c$. The model also contains a gauge singlet S , which triggers the breaking of G_{PS} , as well as an $SU(4)_C$ **6**-plet G , which splits into g_a^c and \bar{g}_a^c under G_{SM} and gives [26] superheavy masses to d_{Ha}^c and \bar{d}_{Ha}^c . In particular, G can be represented by an antisymmetric 4×4 matrix as follows

$$G = \begin{pmatrix} \varepsilon_{abc} g_c^c & \bar{g}_a^c \\ -\bar{g}_a^c & 0 \end{pmatrix} \Rightarrow \bar{G} = \begin{pmatrix} \varepsilon_{abc} \bar{g}_c^c & g_a^c \\ -g_a^c & 0 \end{pmatrix}. \quad (2.3)$$

Here \bar{G} is the dual tensor of G , defined by $\bar{G}^{IJ} = \varepsilon^{IJKL} G_{KL}$ which transforms under $SU(4)_C$ as $U_C^* \bar{G} U_C^\dagger$. Also $\varepsilon^{IJKL} = \varepsilon_{IJKL} [\varepsilon_{abc}]$ is the well-known antisymmetric tensor acting on the $SU(4)_C$ [$SU(3)_C$] indices with $\varepsilon_{1234} = 1$ [$\varepsilon_{123} = 1$]. In the simplest realization of this model [19, 26], the electroweak doublets H_u and H_d , which couple to the up and down quark superfields respectively, are exclusively contained in the bidoublet superfield \mathbb{H} , which can be written as

$$\mathbb{H} = \begin{pmatrix} H_u & H_d \end{pmatrix} = \begin{pmatrix} H_u^+ & H_d^0 \\ H_u^0 & H_d^- \end{pmatrix}. \quad (2.4)$$

In addition to G_{PS} , the model possesses two global $U(1)$ symmetries, namely a PQ and an R symmetry, as well as a discrete \mathbb{Z}_2^{mp} symmetry (‘matter parity’) under which F , F^c change sign. The last symmetry forbids undesirable mixings of F and \mathbb{H} and/or F^c and H^c . The imposed $U(1)$ R symmetry, $U(1)_R$, guarantees the linearity of the superpotential w.r.t the singlet S . Although S does not play the role of the inflaton in our case – in contrast to the case of HI – we explicitly checked that the presence of a quadratic S^2 term would lead to the violation of the stability of the inflationary trajectory. Finally the $U(1)$ PQ symmetry, $U(1)_{\text{PQ}}$, assists us to generate the μ -term of the MSSM. Although this goal could be easily achieved [38] by coupling S to \mathbb{H}^2 and using the fact that S , after gravity-mediated SUSY breaking, develops a v.e.v, we here prefer to follow Ref. [19, 27] imposing a PQ symmetry on the superpotential and introducing a pair of gauge singlet superfields P and \bar{P} . The

SUPER-FIELDS	REPRESE- NTATIONS UNDER G_{PS}	TRASFOR- MATIONS UNDER G_{PS}	DECOMPO- SITIONS UNDER G_{SM}	GLOBAL CHARGES		
				R	PQ	\mathbb{Z}_2^{mp}
MATTER SUPERFIELDS						
F_i	$(\mathbf{4}, \mathbf{2}, \mathbf{1})$	$F_i U_L^\dagger U_C^\top$	$Q_{ia}(\mathbf{3}, \mathbf{2}, 1/6)$ $L_i(\mathbf{1}, \mathbf{2}, -1/2)$	1	-1	1
F_i^c	$(\bar{\mathbf{4}}, \mathbf{1}, \mathbf{2})$	$U_C^* U_R^* F_i^c$	$u_{ia}^c(\bar{\mathbf{3}}, \mathbf{1}, -2/3)$ $d_{ia}^c(\bar{\mathbf{3}}, \mathbf{1}, 1/3)$ $\nu_i^c(\mathbf{1}, \mathbf{1}, 0)$ $e_i^c(\mathbf{1}, \mathbf{1}, 1)$	1	0	-1
HIGGS SUPERFIELDS						
H^c	$(\bar{\mathbf{4}}, \mathbf{1}, \mathbf{2})$	$U_C^* U_R^* H^c$	$u_{Ha}^c(\bar{\mathbf{3}}, \mathbf{1}, -2/3)$ $d_{Ha}^c(\bar{\mathbf{3}}, \mathbf{1}, 1/3)$ $\nu_H^c(\mathbf{1}, \mathbf{1}, 0)$ $e_H^c(\mathbf{1}, \mathbf{1}, 1)$	0	0	0
\bar{H}^c	$(\mathbf{4}, \mathbf{1}, \mathbf{2})$	$\bar{H}^c U_R^\top U_C^\top$	$\bar{u}_{Ha}^c(\mathbf{3}, \mathbf{1}, 2/3)$ $\bar{d}_{Ha}^c(\mathbf{3}, \mathbf{1}, -1/3)$ $\bar{\nu}_H^c(\mathbf{1}, \mathbf{1}, 0)$ $\bar{e}_H^c(\mathbf{1}, \mathbf{1}, -1)$	0	0	0
S	$(\mathbf{1}, \mathbf{1}, \mathbf{1})$	S	$S(\mathbf{1}, \mathbf{1}, 0)$	2	0	0
G	$(\mathbf{6}, \mathbf{1}, \mathbf{1})$	$U_C G U_C^\top$	$\bar{g}_a^c(\mathbf{3}, \mathbf{1}, -1/3)$ $g_a^c(\bar{\mathbf{3}}, \mathbf{1}, 1/3)$	2	0	0
IH	$(\mathbf{1}, \mathbf{2}, \mathbf{2})$	$U_L I H U_R^\top$	$H_u(\mathbf{1}, \mathbf{2}, 1/2)$ $H_d(\mathbf{1}, \mathbf{2}, -1/2)$	0	1	0
P	$(\mathbf{1}, \mathbf{1}, \mathbf{1})$	P	$P(\mathbf{1}, \mathbf{1}, 0)$	1	-1	0
\bar{P}	$(\mathbf{1}, \mathbf{1}, \mathbf{1})$	\bar{P}	$\bar{P}(\mathbf{1}, \mathbf{1}, 0)$	0	1	0

Table 1: The representations, the transformations under G_{PS} , the decompositions under G_{SM} as well as the extra global charges of the superfields of our model. Here $U_C \in SU(4)_C$, $U_L \in SU(2)_L$, $U_R \in SU(2)_R$ and \top , \dagger and $*$ stand for the transpose, the hermitian conjugate and the complex conjugate of a matrix respectively.

PQ breaking occurs at an intermediate scale through the v.e.v.s of P , \bar{P} , and the μ -term is generated via a non-renormalizable coupling of P and IH . We do not adopt here the resolution to the μ -problem suggested in Ref. [38], since it introduces a renormalizable term which creates (i) a decay channel of the inflaton which leads to a high reheating temperature in conflict with the \tilde{G} constraint and (ii) a tachyonic instability in the $H_u - H_d$ system during non-MHI – as occurring in Ref. [11]. Lifting both shortcomings requires an unnaturally small value for the relevant coupling constant in our scenario (of order 10^{-6} or so), which is certainly undesirable. Following Ref. [19], we introduce into the scheme quartic (non-renormalizable) superpotential couplings of \bar{H}^c to F_i^c , which generate intermediate-scale masses for the ν_i^c and, thus, masses for the light neutrinos, ν_i , via the seesaw mechanism. Moreover,

these couplings allow for the decay of the inflaton into RH neutrinos, ν_i^c , leading to a reheating temperature consistent with the \tilde{G} constraint with more or less natural values of the parameters. As shown finally in Ref. [19], the proton turns out to be practically stable in this model.

The superpotential W of our model splits into three parts:

$$W = W_{\text{MSSM}} + W_{\text{PQ}} + W_{\text{HPS}}, \quad (2.5)$$

where W_{MSSM} is the part of W which contains the usual terms – except for the μ term – of the MSSM, supplemented by Yukawa interactions among the left-handed leptons and ν_i^c :

$$W_{\text{MSSM}} = y_{ij} F_i \mathbb{H} F_j^c = y_{ij} \left(H_d^\top \varepsilon L_i e_j^c - H_u^\top \varepsilon L_i \nu_j^c + H_d^\top \varepsilon Q_{ia} d_{ja}^c - H_u^\top \varepsilon Q_{ia} u_{ja}^c \right), \quad \text{with } \varepsilon = \begin{pmatrix} 0 & 1 \\ -1 & 0 \end{pmatrix}. \quad (2.6)$$

Here $Q_{ia} = \begin{pmatrix} u_{ia} & d_{ia} \end{pmatrix}^\top$ and $L_i = \begin{pmatrix} \nu_i & e_i \end{pmatrix}^\top$ are the i -th generation $SU(2)_L$ doublet LH quark and lepton superfields respectively. Summation over repeated color and generation indices is also assumed. Obviously the model predicts Yukawa unification at M_{GUT} since the third family fermion masses originate from a unique term in the underlying GUT. It is shown [39,40] that exact Yukawa unification combined with non-universalities in the gaugino sector and/or the scalar sector can become consistent with a number of phenomenological and cosmological low-energy requirements. The present model can be augmented [37] with other Higgs fields so that H_u and H_d are not exclusively contained in \mathbb{H} but receive subdominant contributions from other representations too. As a consequence, a moderate violation of the exact Yukawa unification can be achieved, allowing for an acceptable low-energy phenomenology, even with universal boundary conditions for the soft SUSY breaking terms. However, here we prefer to work with the simplest version of the PS model.

The second term in the *right hand side* (RHS) of Eq. (2.5), W_{PQ} , is the part of W which is relevant for the spontaneous breaking of $U(1)_{\text{PQ}}$ and the generation of the μ term of the MSSM. It is given by

$$W_{\text{PQ}} = \lambda_{\text{PQ}} \frac{P^2 \bar{P}^2}{M_S} - \lambda_\mu \frac{P^2}{2M_S} \text{Tr} \left(\mathbb{H} \varepsilon \mathbb{H}^\top \varepsilon \right), \quad (2.7)$$

where $M_S \simeq 5 \cdot 10^{17}$ GeV is the String scale. The scalar potential, which is generated by the first term in the RHS of Eq. (2.7), after gravity-mediated SUSY breaking is studied in Ref. [19,27]. For a suitable choice of parameters, the minimum lies at $|\langle P \rangle| = |\langle \bar{P} \rangle| \sim \sqrt{m_{3/2} M_S}$. Hence, the PQ symmetry breaking scale is of order $\sqrt{m_{3/2} M_S} \simeq (10^{10} - 10^{11})$ GeV and the μ -term of the MSSM is generated from the second term of the RHS of Eq. (2.7) as follows:

$$-\lambda_\mu \frac{\langle P \rangle^2}{2M_S} \text{Tr} \left(\mathbb{H} \varepsilon \mathbb{H}^\top \varepsilon \right) = \mu H_d^\top \varepsilon H_u \Rightarrow \mu \simeq \lambda_\mu \frac{\langle P \rangle^2}{M_S}, \quad (2.8)$$

which is of the right magnitude if $\lambda_\mu \sim (0.001 - 0.01)$. Let us note that V_{PQ} has an additional local minimum at $P = \bar{P} = 0$, which is separated from the global PQ minimum by a sizable potential barrier, thus preventing transitions from the trivial to the PQ vacuum. Since this situation persists at all cosmic temperatures after reheating, we are obliged to assume that, after the termination of non-MHI, the system emerges with the appropriate combination of initial conditions so that it lies [41] in the PQ vacuum.

Finally, the third term in the RHS of Eq. (2.5), W_{HPS} , is the part of W which is relevant for non-MHI, the spontaneous breaking of G_{PS} and the generation of intermediate Majorana [superheavy] masses for ν_i^c [d_H^c and \bar{d}_H^c]. It takes the form

$$W_{\text{HPS}} = \lambda S \left(\bar{H}^c H^c - M_{\text{PS}}^2 \right) + \lambda_H H^c \mathbb{H}^\top G \varepsilon H^c + \lambda_{\bar{H}} \bar{H}^c \bar{G} \varepsilon \bar{H}^{c\top} + \lambda_{i\nu^c} \frac{(\bar{H}^c F_i^c)^2}{M_S}, \quad (2.9)$$

where M_{PS} is a superheavy mass scale related to M_{GUT} – see Sec. 3.2. The parameters λ and M_{PS} can be made positive by field redefinitions. It is worth emphasizing that our inflationary model is totally tied on renormalizable superpotential terms, contrary to the model of shifted HI [19], where a non-renormalizable term added in the RHS of Eq. (2.9) plays a crucial role in the inflationary dynamics.

Suppressing henceforth the color indices, we can express W_{HPS} in terms of the components of the various superfields. We find

$$\begin{aligned} W_{\text{HPS}} &= \lambda S (\nu_H^c \bar{\nu}_H^c + e_H^c \bar{e}_H^c + u_H^c \bar{u}_H^c + d_H^c \bar{d}_H^c - M_{\text{PS}}^2) \\ &- 2\lambda_H (\nu_H^c d_H^c - e_H^c u_H^c) \bar{g}^c + 2\lambda_H u_H^c d_H^c g^c \\ &- 2\lambda_{\bar{H}} (\bar{\nu}_H^c \bar{d}_H^c - \bar{e}_H^c \bar{u}_H^c) g^c + 2\lambda_{\bar{H}} \bar{u}_H^c \bar{d}_H^c \bar{g}^c \\ &+ \lambda_{i\nu^c} (\bar{e}_H^c e_i^c + \bar{d}_H^c d_i^c - \bar{\nu}_H^c \nu_i^c - \bar{u}_H^c u_i^c)^2 / M_S. \end{aligned} \quad (2.10)$$

Let us note in passing that the combination of two [three] color-charged objects in a term involves a contraction of the color indices with the symmetric [antisymmetric] invariant tensor δ_{ab} [ε_{abc}], e.g., $u_H^c \bar{u}_H^c = \delta_{ab} u_{Ha}^c \bar{u}_{Hb}^c$ [$u_H^c d_H^c g^c = \varepsilon_{abc} u_{Ha}^c d_{Hb}^c g_c^c$].

According to the general recipe [3, 10], the implementation of non-MHI within SUGRA requires the adoption of a frame function, Ω , related to the Kähler potential, K , as follows

$$\Omega = -3e^{-K/3m_{\text{P}}^2} = -3 + \frac{H^{c\dagger} H^c}{m_{\text{P}}^2} + \frac{\bar{H}^c \bar{H}^{c\dagger}}{m_{\text{P}}^2} + \frac{\text{Tr}(G^\dagger G)}{2m_{\text{P}}^2} + \frac{|S|^2}{m_{\text{P}}^2} - k_S \frac{|S|^4}{m_{\text{P}}^4} - \frac{3k_H}{2m_{\text{P}}^2} (\bar{H}^c H^c + \text{h.c.}), \quad (2.11)$$

where the complex scalar components of the superfields H^c, \bar{H}^c, G and S are denoted by the same symbol and the coefficients k_S and k_H are taken real. It is clear from Eq. (2.11) that we adopt the standard quadratic non-minimal coupling for Higgs-inflaton, which respects the gauge and the global symmetries of the model. We also added the fifth term in the RHS of Eq. (2.11) in order to cure the tachyonic mass problem encountered in similar models [3, 10] – see Sec. 3.1. In terms of the components of the various fields, K in Eq. (2.11) reads

$$K = -3m_{\text{P}}^2 \ln \left(1 - \frac{\phi^\alpha \phi^{*\alpha}}{3m_{\text{P}}^2} + k_S \frac{|S|^4}{3m_{\text{P}}^4} + \frac{k_H}{2m_{\text{P}}^2} (\nu_H^c \bar{\nu}_H^c + e_H^c \bar{e}_H^c + u_H^c \bar{u}_H^c + d_H^c \bar{d}_H^c + \text{h.c.}) \right) \quad (2.12)$$

with $\phi^\alpha = \nu_H^c, \bar{\nu}_H^c, e_H^c, \bar{e}_H^c, u_H^c, \bar{u}_H^c, d_H^c, \bar{d}_H^c, g^c, \bar{g}^c, S$ and summation over the repeated Greek indices – e.g. α and β – is implied

In the limit where m_{P} tends to infinity, we can obtain the SUSY limit, V_{SUSY} , of the SUGRA potential, \widehat{V}_{HF} – see Sec. 3. Assuming that the SM non-singlet components vanish, V_{SUSY} turns out to be

$$V_{\text{SUSY}} = \lambda^2 |(\bar{\nu}_H^c \nu_H^c - M_{\text{PS}}^2)|^2 + \lambda^2 |S|^2 (|\nu_H^c|^2 + |\bar{\nu}_H^c|^2). \quad (2.13)$$

On the other hand, assuming minimal gauge kinetic functions, the D-term scalar potential V_{HD} of the PS Higgs fields takes the form

$$V_{\text{HD}} = \frac{g^2}{2} \sum_{a=1}^{15} \left(\bar{H}^{c*} T_C^a \bar{H}^{c\dagger} - H^{c\dagger} T_C^{a*} H^c \right)^2 + \frac{g^2}{2} \sum_{m=1}^3 \left(\bar{H}^{c*} T_R^m \bar{H}^{c\dagger} - H^{c\dagger} T_R^{m*} H^c \right)^2, \quad (2.14)$$

where g is the (unified) gauge coupling constant of G_{PS} . In terms of the components of \bar{H}^c and H^c , V_{HD} reads:

$$\begin{aligned} V_{\text{HD}} &= \frac{g^2}{8} \left[(\bar{\nu}_H^{c*} \bar{e}_H^c + \bar{\nu}_H^c \bar{e}_H^{c*} - \nu_H^{c*} e_H^c - \nu_H^c e_H^{c*})^2 - (\nu_H^c e_H^{c*} - \nu_H^{c*} e_H^c + \bar{\nu}_H^c \bar{e}_H^{c*} - \bar{\nu}_H^{c*} \bar{e}_H^c)^2 \right. \\ &+ (\bar{\nu}_H^{c*} \bar{u}_H^c + \bar{\nu}_H^c \bar{u}_H^{c*} - \nu_H^{c*} u_H^c - \nu_H^c u_H^{c*})^2 - (\nu_H^{c*} u_H^c - \nu_H^c u_H^{c*} - \bar{\nu}_H^{c*} \bar{u}_H^c + \bar{\nu}_H^c \bar{u}_H^{c*})^2 \\ &\left. + \frac{3}{2} (|\nu_H^c|^2 - |\bar{\nu}_H^c|^2)^2 + (|\bar{\nu}_H^c|^2 - |\nu_H^c|^2)^2 + \dots \right]. \end{aligned} \quad (2.15)$$

Here the first line includes contributions arising from the sum over the $SU(2)_R$ generators T_R^1 and T_R^2 in Eq. (2.14), which are the well-known Pauli matrices. The second line includes contributions from the sum over the $SU(4)_C$ generators T^{7+2a} [T^{8+2a}] ($a = 1, 2, 3$) with $1/2$ [$1/2$] and $-i/2$ [$i/2$] in the $a4$ [$4a$] entries respectively and zero everywhere else, and the third for T_C^{15} and T_R^3 . The ellipsis represents terms including exclusively the SM non-singlet directions of \bar{H}^c and H^c . Vanishing of the D-terms is achieved for $|\bar{\nu}_H^c| = |\nu_H^c|$ with the other components of \bar{H}^c and H^c frozen at zero. Restricting ourselves to the D-flat direction, from V_{SUSY} in Eq. (2.13) we find that the SUSY vacuum lies at

$$\langle S \rangle \simeq 0 \quad \text{and} \quad |\langle \nu_H^c \rangle| = |\langle \bar{\nu}_H^c \rangle| = M_{\text{PS}}. \quad (2.16)$$

Therefore, W_{HPS} leads to a spontaneous breaking of G_{PS} . The same superpotential, W_{HPS} , also gives rise to a stage of non-MHI as analyzed in Sec. 3. Indeed, along the D-flat direction $|\nu_H^c| = |\bar{\nu}_H^c| \gg M_{\text{PS}}$ and $S = 0$, V_{SUSY} tends to a quartic potential and so, W_{HPS} can be employed in conjunction with K in Eq. (2.11) for the realization of non-MHI along the lines of Ref. [10].

It should be mentioned that soft SUSY breaking and instanton effects explicitly break $U(1)_R \times U(1)_{\text{PQ}}$ to $\mathbb{Z}_2 \times \mathbb{Z}_6$. The latter symmetry is spontaneously broken by $\langle P \rangle$ and $\langle \bar{P} \rangle$. This would lead to a domain wall problem if the PQ transition took place after non-MHI. However, as we already mentioned above, $U(1)_{\text{PQ}}$ is assumed already broken before or during non-MHI. The final unbroken symmetry of the model is $G_{\text{SM}} \times \mathbb{Z}_2^{\text{mp}}$.

3 THE INFLATIONARY SCENARIO

We below outline the salient features of our inflationary scenario (Sec. 3.1) and then, we present its predictions in Sec. 3.3, calculating a number of observable quantities introduced in Sec. 3.2.

3.1 STRUCTURE OF THE INFLATIONARY ACTION

Following the conventions of Ref. [11], we write the action of our model in the *Jordan frame* (JF) as follows:

$$S_{\text{HI}} = \int d^4x \sqrt{-g} \left(\frac{1}{6} m_{\text{P}}^2 \Omega \mathcal{R} + m_{\text{P}}^2 \Omega_{\alpha\bar{\beta}} \partial_\mu \phi^\alpha \partial^\mu \phi^{*\bar{\beta}} - V_{\text{HI}} + \dots \right), \quad (3.1)$$

where $\Omega_{\alpha\bar{\beta}} = \Omega_{,\phi^\alpha \phi^{\bar{\beta}}}$ and ϕ^α are identified below Eq. (2.12). The ellipsis represents terms arising from the covariant derivatives $D_\mu H^c$ and $D_\mu \bar{H}^c$, and terms that include the on-shell auxiliary axial-vector field [3, 11], which turn out to be irrelevant for our analysis below. Here $V_{\text{HI}} = \Omega^2 \widehat{V}_{\text{HF}}/9 + V_{\text{HD}}$, with \widehat{V}_{HF} being the *Einstein frame* (EF) F-term SUGRA scalar potential, which is obtained from W_{HPS} in Eq. (2.10) – without the last term of the RHS – and K in Eq. (2.12) by applying [42]

$$\widehat{V}_{\text{HF}} = e^{K/m_{\text{P}}^2} \left(K^{\alpha\bar{\beta}} F_\alpha F_{\bar{\beta}} - 3 \frac{|W_{\text{HPS}}|^2}{m_{\text{P}}^2} \right) \quad \text{and} \quad K_{\alpha\bar{\beta}} = \frac{\partial^2 K}{\partial \phi^\alpha \partial \phi^{*\bar{\beta}}}, \quad (3.2)$$

with $K^{\bar{\beta}\alpha} K_{\alpha\bar{\gamma}} = \delta_{\bar{\gamma}}^{\bar{\beta}}$ and $F_\alpha = W_{\text{HPS},\phi^\alpha} + K_{,\phi^\alpha} W_{\text{HPS}}/m_{\text{P}}^2$.

If we parameterize the SM neutral components of H^c and \bar{H}^c by

$$\nu_H^c = h e^{i\theta} \cos \theta_\nu / \sqrt{2} \quad \text{and} \quad \bar{\nu}_H^c = h e^{i\bar{\theta}} \sin \theta_\nu / \sqrt{2}, \quad (3.3)$$

we can easily deduce from Eq. (2.15) that a D-flat direction occurs at

$$\theta = \bar{\theta} = 0, \quad \theta_\nu = \pi/4 \quad \text{and} \quad e_H^c = \bar{e}_H^c = u_H^c = \bar{u}_H^c = d_H^c = \bar{d}_H^c = g^c = \bar{g}^c = 0. \quad (3.4)$$

Along this direction, V_{HD} in Eq. (2.15) vanishes and so, $\widehat{V}_{\text{HI}} = \widehat{V}_{\text{HF}}$ takes the form

$$\widehat{V}_{\text{HI0}} = m_{\text{P}}^4 \frac{\lambda^2 (x_h^2 - 4m_{\text{PS}}^2)^2}{16f^2} \quad \text{with} \quad f = -\frac{\Omega}{3} = 1 + c_{\mathcal{R}} x_h^2 \quad \text{and} \quad c_{\mathcal{R}} = -\frac{1}{6} + \frac{k_H}{4}. \quad (3.5)$$

Here $m_{\text{PS}} = M_{\text{PS}}/m_{\text{P}}$ and $x_h = h/m_{\text{P}}$. From Eq. (3.5), we can verify that for $c_{\mathcal{R}} \gg 1$, S_{HI} in Eq. (3.1) takes a form suitable for the realization of non-MHI: the terms in the ellipsis vanish, and more importantly \widehat{V}_{HI} develops a plateau since $m_{\text{PS}} \ll 1$ – see Sec. 3.2. The (almost) constant potential energy density \widehat{V}_{HI0} and the corresponding Hubble parameter \widehat{H}_{HI0} along the trajectory in Eq. (3.4) are given by

$$\widehat{V}_{\text{HI0}} = \frac{\lambda^2 h^4}{16f^2} \simeq \frac{\lambda^2 m_{\text{P}}^4}{16c_{\mathcal{R}}^2} \quad \text{and} \quad \widehat{H}_{\text{HI0}} = \frac{\widehat{V}_{\text{HI0}}^{1/2}}{\sqrt{3}m_{\text{P}}} \simeq \frac{\lambda m_{\text{P}}}{4\sqrt{3}c_{\mathcal{R}}}. \quad (3.6)$$

We next proceed to check the stability of the trajectory in Eq. (3.4) w.r.t the fluctuations of the various fields. To this end, we expand them in real and imaginary parts as follows

$$X = \frac{x_1 + ix_2}{\sqrt{2}}, \quad \bar{X} = \frac{\bar{x}_1 + i\bar{x}_2}{\sqrt{2}} \quad \text{where} \quad X = e_H^c, u_H^c, d_H^c, g^c \quad \text{and} \quad x = e, u, d, g. \quad (3.7)$$

respectively. Notice that the field S can be rotated to the real axis via a suitable R transformation. Since along the trajectory in Eq. (3.4) the various fields, X and \bar{X} , are confined to zero, the radial parametrization employed in Eq. (3.3) is not convenient here. Performing a Weyl transformation as described in detail in Ref. [11], we obtain

$$S_{\text{HI}} = \int d^4x \sqrt{-\widehat{g}} \left(-\frac{1}{2} m_{\text{P}}^2 \widehat{\mathcal{R}} + \begin{pmatrix} \partial_\mu \nu_H^{c*} & \partial_\mu \bar{\nu}_H^{c*} \end{pmatrix} \frac{M_K}{f^2} \begin{pmatrix} \partial^\mu \nu_H^c \\ \partial^\mu \bar{\nu}_H^c \end{pmatrix} + \frac{1}{2f} \sum_\chi \partial_\mu \chi \partial^\mu \chi - \widehat{V}_{\text{HI}} \right),$$

where $M_K = \begin{pmatrix} \kappa & \bar{\kappa} \\ \bar{\kappa} & \kappa \end{pmatrix}$, $\bar{\kappa} = 3c_{\mathcal{R}}^2 x_h^2$, $\kappa = f + \bar{\kappa}$ and $\widehat{V}_{\text{HI}} = \widehat{V}_{\text{HF}} + V_{\text{HD}}/f^2$. (3.8)

In deriving this result, we take into account that $f_{,\chi} \ll f_{,h}$ with $\chi = S, x_1, x_2, \bar{x}_1$ and \bar{x}_2 , and keep only terms up to quadratic order in the fluctuations χ and their derivatives. To canonically normalize the fields ν_H^c and $\bar{\nu}_H^c$, we have to diagonalize the matrix M_K . This can be realized via a similarity transformation involving an orthogonal matrix U_K as follows:

$$U_K M_K U_K^\top = \text{diag}(\bar{f}, f), \quad \text{where} \quad \bar{f} = f + 6c_{\mathcal{R}}^2 x_h^2 \quad \text{and} \quad U_K = \frac{1}{\sqrt{2}} \begin{pmatrix} 1 & 1 \\ -1 & 1 \end{pmatrix}. \quad (3.9)$$

By inserting $\mathbf{1} = U_K U_K^\top = U_K^\top U_K$ on the left and the right of M_K , we bring the second term of the parenthesis in the RHS of Eq. (3.8) into the form

$$\frac{1}{2f^2} \left(\bar{f} \left(\partial_\mu h \partial^\mu h + \frac{1}{2} h^2 \partial_\mu \theta_+ \partial^\mu \theta_+ \right) + f h^2 \left(\frac{1}{2} \partial_\mu \theta_- \partial^\mu \theta_- + \partial_\mu \theta_\nu \partial^\mu \theta_\nu \right) \right), \quad (3.10)$$

along the trajectory in Eq. (3.4). Here $\theta_\pm = (\bar{\theta} \pm \theta)/\sqrt{2}$. Consequently, we can introduce the EF canonically normalized fields, $\widehat{h}, \widehat{\theta}_+, \widehat{\theta}_-, \widehat{\theta}_\nu$ and $\widehat{\chi}$, as follows – cf. Ref. [3, 10]

$$\frac{d\widehat{h}}{dh} = J = \frac{\sqrt{\bar{f}}}{f} = \sqrt{\frac{1}{f} + \frac{6c_{\mathcal{R}}^2 x_h^2}{f^2}}, \quad \widehat{\theta}_+ = \frac{Jh\theta_+}{\sqrt{2}}, \quad \widehat{\theta}_- = \frac{h\theta_-}{\sqrt{2f}}, \quad \widehat{\theta}_\nu = \frac{h\theta_\nu}{\sqrt{f}} \quad \text{and} \quad \widehat{\chi} = \frac{\chi}{\sqrt{f}}. \quad (3.11)$$

Taking into account the approximate expressions for \dot{h} – where the dot denotes derivation w.r.t the cosmic time, $t - J$ and the slow-roll parameters $\widehat{\epsilon}, \widehat{\eta}$, which are displayed in Sec. 3.2, we can verify that, during a stage of slow-roll non-MHI, $\dot{\widehat{\theta}}_+ \simeq Jh\dot{\theta}_+/\sqrt{2}$ since $Jh \simeq \sqrt{6}m_{\text{P}}$, $\dot{\widehat{\theta}}_- \simeq h\dot{\theta}_-/\sqrt{2f}$ and $\dot{\widehat{\theta}}_\nu \simeq h\dot{\theta}_\nu/\sqrt{f}$ since $h/\sqrt{f} \simeq m_{\text{P}}/\sqrt{c_{\mathcal{R}}}$, and finally $\dot{\widehat{\chi}} \simeq \dot{\chi}/\sqrt{f}$. For the latter, the quantity

$\dot{f}/f^{3/2}$, involved in relating $\hat{\chi}$ to $\dot{\chi}$, turns out to be negligibly small, since $\dot{f}/f^{3/2} = f_{,h}\dot{h}/f^{3/2} = -\lambda\sqrt{\epsilon|\eta|}m_{\text{P}}/2\sqrt{3}c_{\mathcal{R}}$. Therefore the action in Eq. (3.8) takes the form

$$S_{\text{HI}} = \int d^4x \sqrt{-\hat{g}} \left(-\frac{1}{2}m_{\text{P}}^2\hat{\mathcal{R}} + \frac{1}{2}\hat{g}^{\mu\nu} \sum_{\phi} \partial_{\mu}\hat{\phi}\partial_{\nu}\hat{\phi} - \hat{V}_{\text{HI}} \right), \quad \text{with } \hat{V}_{\text{HI}} = \hat{V}_{\text{HF}} + \frac{V_{\text{HD}}}{f^2} \quad (3.12)$$

where ϕ stands for $h, \theta_+, \theta_-, \theta_{\nu}, x_1, x_2, \bar{x}_1, \bar{x}_2$ and S .

Having defined the canonically normalized scalar fields, we can proceed in investigating the stability of the inflationary trajectory of Eq. (3.4). To this end, we expand \hat{V}_{HI} in Eq. (3.12) to quadratic order in the fluctuations around the direction of Eq. (3.4), as we describe in detail in Sec. A.1. In Table 2 we list the eigenvalues of the masses-squared matrices $M_{\alpha\beta}^2 = \left(\partial^2\hat{V}_{\text{HI}}/\partial\hat{\chi}_{\alpha}\partial\hat{\chi}_{\beta} \right)$ with $\chi_{\alpha} = \theta_+, \theta_-, \theta_{\nu}, x_{1,2}, \bar{x}_{1,2}$ and S involved in the expansion of \hat{V}_{HI} . We arrange our findings into three groups: the SM singlet sector, $S - \nu_H^c - \bar{\nu}_H^c$, the sector with the u_H^c, \bar{u}_H^c and the e_H^c, \bar{e}_H^c fields which are related with the broken generators of G_{PS} and the sector with the d_H^c, \bar{d}_H^c and the g^c, \bar{g}^c fields.

As we observe from the relevant eigenvalues of the mass-squared matrices, no instability – as the one found in Ref. [11] – arises in the spectrum. In particular, it is evident that $k_S \gtrsim 1$ assists us to achieve $m_S^2 > 0$ – in accordance with the results of Ref. [10]. Moreover, the D-term contributions to $m_{\hat{\theta}_{\nu}}^2$ and $m_{\hat{u}^-}^2$ – proportional to the gauge coupling constant $g \simeq 0.7$ – ensure the positivity of these masses squared. Finally the masses that the scalars $\hat{d}_{1,2}$ acquire from the second and third term of the RHS of Eq. (2.9) lead to the positivity of $m_{\hat{d}_2}^2$ for λ_H of order unity. We have also numerically verified that the masses of the various scalars remain greater than the Hubble parameter during the last 50 – 60 e-foldings of non-MHI, and so any inflationary perturbations of the fields other than the inflaton are safely eliminated.

In Table 2 we also present the masses squared of the gauge bosons, chiral fermions and gauginos of the model along the direction of Eq. (3.4). The mass spectrum is necessary in order to calculate the one-loop radiative corrections. Let us stress here that the non-vanishing values of ν_H^c and $\bar{\nu}_H^c$ trigger the spontaneous breaking of G_{PS} to G_{SM} . In particular we have the following pattern of symmetry breaking

$$SU(4)_{\text{C}} \times SU(2)_{\text{R}} \rightarrow SU(3)_{\text{C}} \times U(1)_{\text{Y}}.$$

Therefore, 9 of the 18 generators of $SU(4)_{\text{C}} \times SU(2)_{\text{R}}$ are broken, leading to 9 Goldstone bosons which are “eaten” by the 9 gauge bosons which become massive. As a consequence, 36 *degrees of freedom* (d.o.f) of the spectrum before the spontaneous breaking (18 d.o.f corresponding to 8 complex scalars, $u_{H_a}^c, \bar{u}_{H_a}^c, e_H^c$ and \bar{e}_H^c , and 2 real scalars, θ and $\bar{\theta}$, and 18 d.o.f corresponding to 9 massless gauge bosons, $A_{\text{C}}^9 - A_{\text{C}}^{14}, A_{\text{R}}^1, A_{\text{R}}^2$ and A^{\perp}) of G_{PS} are redistributed as follows: 9 d.o.f are associated with the real propagating scalars (θ_+, x_{1-} and x_{2+} with $x = u^a$ and e) whereas the residual 9 d.o.f combine together with the 18 d.o.f of the initially massless gauge bosons to make massive the following combinations of them $A_{\text{C}}^{a\pm}, A_{\text{R}}^{\pm}$ and A^{\perp} – see Sec. A.2 of Appendix A.

From Table 2 we can deduce that the numbers of bosonic and fermionic d.o.f in each sector are equal. Indeed in the $S - \nu_H^c - \bar{\nu}_H^c$ sector, we obtain 10 bosonic d.o.f and 10 fermionic d.o.f. Note that we consider S as a complex field and we take into account the 1 d.o.f of h which is not perturbed in the expansion of Eq. (A.1). Similarly in the $u_H^c - \bar{u}_H^c$ and $e_H^c - \bar{e}_H^c$ [$d_H^c - \bar{d}_H^c$ and $g^c - \bar{g}^c$] sector we obtain 32 [24] bosonic d.o.f and an equal number of fermionic d.o.f. Note also that the spectrum contains a massless fermion which must be present due to the spontaneous SUSY breaking caused by the tree-level potential energy density in Eq. (3.6).

The 8 Goldstone bosons, associated with the modes x_{1+} and x_{2-} with $x = u^a$ and e , are not exactly massless since $\hat{V}_{\text{HI},h} \neq 0$ – contrary to the situation of Ref. [19] where the direction with non vanishing

FIELDS	MASSES SQUARED	EIGENSTATES
THE $S - \nu_H^c - \bar{\nu}_H^c$ SECTOR		
2 real scalars	$m_{\hat{\theta}_\nu}^2 = m_{\mathbb{P}}^2 x_h^2 (2\lambda^2(x_h^2 - 6) + 15g^2 f) / 24f^2$	$\hat{\theta}_\nu$
	$m_{\hat{\theta}_+}^2 = \lambda^2 m_{\mathbb{P}}^4 x_h^2 (1 + 6c_{\mathcal{R}}) / 12J^2 f^3 \simeq 4\hat{H}_{\text{HI}}^2$	$\hat{\theta}_+$
1 complex scalar	$m_{\hat{S}}^2 = \lambda^2 m_{\mathbb{P}}^2 x_h^2 (12 + x_h^2 \bar{f}) (6k_S f - 1) / 6f^2 \bar{f}$	\hat{S}
2 gauge bosons	$m_{\perp}^2 = 5g^2 m_{\mathbb{P}}^2 x_h^2 / 8f, m_{\parallel}^2 = 0$	A^\perp, A^\parallel
4 Weyl fermions	$m_{\hat{\psi}_{S\nu}}^2 = \lambda^2 m_{\mathbb{P}}^2 x_h^2 / 2\bar{f} f^2$	$\hat{\psi}_{S\nu\pm}$
	$m_{\perp}^2 = 5g^2 m_{\mathbb{P}}^2 x_h^2 / 8f$	$\lambda^\perp, \hat{\psi}_{\nu-}$
1 Majorana fermion	$m_{\parallel}^2 = 0$	$\lambda^\parallel, \hat{\psi}_{\nu+}$
THE $u_{H_a}^c - \bar{u}_{H_a}^c$ ($a = 1, 2, 3$) AND $e_H^c - \bar{e}_H^c$ SECTORS		
2(3 + 1) real scalars	$m_{\hat{u}_-}^2 = m_{\mathbb{P}}^2 x_h^2 (\lambda^2(x_h^2 - 3) + 3g^2 f) / 12f^2$	$\hat{u}_{1-}^a, \hat{u}_{2+}^a,$
	$m_{\hat{e}_-}^2 = m_{\hat{u}_-}^2$	$\hat{e}_{1-}, \hat{e}_{2+}$
2(3 + 1) gauge bosons	$m_{\pm}^2 = g^2 m_{\mathbb{P}}^2 x_h^2 / 4f$	A_C^{\pm}, A_R^{\pm}
4(3 + 1) Weyl fermions	$m_{\pm}^2 = g^2 m_{\mathbb{P}}^2 x_h^2 / 4f$	$\lambda_C^{\pm}, \psi_u^a, \psi_{\bar{u}}^a$
		$\lambda_R^{\pm}, \psi_e, \psi_{\bar{e}}$
THE $d_{H_a}^c - \bar{d}_{H_a}^c$ AND $g_a^c - \bar{g}_a^c$ ($a = 1, 2, 3$) SECTORS		
3 · 8 real scalars	$m_{\hat{g}}^2 = m_{\mathbb{P}}^2 x_h^2 (\lambda^2 x_h^2 + 24\lambda_{\bar{H}}^2 f) / 24f^2$	\hat{g}_1^a, \hat{g}_2^a
	$m_{\hat{g}}^2 = m_{\mathbb{P}}^2 x_h^2 (\lambda^2 x_h^2 + 24\lambda_H^2 f) / 24f^2$	\hat{g}_1^a, \hat{g}_2^a
	$m_{\hat{d}_+}^2 = m_{\mathbb{P}}^2 x_h^2 (\lambda^2 + 4\lambda_H^2 f) / 4f^2$	$\hat{d}_{1+}^a, \hat{d}_{2-}^a$
	$m_{\hat{d}_-}^2 = m_{\mathbb{P}}^2 x_h^2 (\lambda^2 (x_h^2 - 3) + 12\lambda_{\bar{H}}^2 f) / 12f^2$	$\hat{d}_{1-}^a, \hat{d}_{2+}^a$
3 · 4 Weyl fermions	$m_{\hat{\psi}_{g_d}}^2 = \lambda_H^2 m_{\mathbb{P}}^2 x_h^2 / f$	$\hat{\psi}_{g_d\pm}^a$
	$m_{\hat{\psi}_{g_{\bar{d}}}}^2 = \lambda_{\bar{H}}^2 m_{\mathbb{P}}^2 x_h^2 / f$	$\hat{\psi}_{g_{\bar{d}}\pm}^a$

Table 2: The mass spectrum of our model along the inflationary trajectory of Eq. (3.4). To avoid very lengthy formulas we neglect terms proportional to $m_{\mathbb{P}S}^2$ and we assume $\lambda_H \simeq \lambda_{\bar{H}}$ for the derivation of the masses of the scalars in the superfields $d_{H_a}^c$ and $\bar{d}_{H_a}^c$. The various eigenstates are defined in Sec. 3.1 and Appendix A.

$\langle \nu_H^c \rangle$ corresponds to a minimum of the potential. These masses turn out to be $m_{x_0} = \lambda m_{\mathbb{P}} x_h / 2f$. On the contrary, the angular parametrization in Eq. (3.3) assists us to isolate the massless mode $\hat{\theta}_-$, in agreement with the analysis of Ref. [3]. In computing below the one-loop radiative corrections, V_{rc} , in our model, we do not treat the residual Goldstone bosons as independent fields, since their associated d.o.f are “eaten” by the massive gauge bosons – for a different point of view, see Ref. [50]. After all, as we expect and verified numerically, V_{rc} has no significant effect on the inflationary dynamics and predictions, since the slope of the inflationary path is generated at the classical level – see the expressions for $\hat{\epsilon}$ and $\hat{\eta}$ below – and no significant running of the relevant parameters occurs – contrary to the SM or next-to-MSSM non-MHI. Employing the well-known Coleman-Weinberg formula [44],

we find

$$V_{\text{rc}} = V_{S\nu_H^c \bar{\nu}_H^c} + V_{u_H^c \bar{u}_H^c e_H^c \bar{e}_H^c} + V_{d_H^c \bar{d}_H^c g^c \bar{g}^c}, \quad (3.13)$$

where the individual contributions, coming from the corresponding sectors of Table 2, are given by

$$\begin{aligned} V_{S\nu_H^c \bar{\nu}_H^c} &= \frac{1}{64\pi^2} \left(m_{\hat{\theta}_\nu}^4 \ln \frac{m_{\hat{\theta}_\nu}^2}{\Lambda^2} + m_{\hat{\theta}_+}^4 \ln \frac{m_{\hat{\theta}_+}^2}{\Lambda^2} + 2m_{\hat{S}}^4 \ln \frac{m_{\hat{S}}^2}{\Lambda^2} \right. \\ &\quad \left. + 3m_{\hat{1}}^4 \ln \frac{m_{\hat{1}}^2}{\Lambda^2} - 4m_{\hat{\psi}_{S\nu+}}^4 \ln \frac{m_{\hat{\psi}_{S\nu+}}^2}{\Lambda^2} - 4m_{\hat{1}}^4 \ln \frac{m_{\hat{1}}^2}{\Lambda^2} \right), \end{aligned} \quad (3.14a)$$

$$V_{u_H^c \bar{u}_H^c e_H^c \bar{e}_H^c} = \frac{4}{64\pi^2} \left(2m_{\hat{u}_-}^4 \ln \frac{m_{\hat{u}_-}^2}{\Lambda^2} + 6m_{\hat{\pm}}^4 \ln \frac{m_{\hat{\pm}}^2}{\Lambda^2} - 8m_{\hat{\pm}}^4 \ln \frac{m_{\hat{\pm}}^2}{\Lambda^2} \right), \quad (3.14b)$$

$$\begin{aligned} V_{d_H^c \bar{d}_H^c g^c \bar{g}^c} &= \frac{3}{64\pi^2} \left(2m_{\hat{g}}^4 \ln \frac{m_{\hat{g}}^2}{\Lambda^2} + 2m_{\hat{g}}^4 \ln \frac{m_{\hat{g}}^2}{\Lambda^2} + 2m_{\hat{d}_+}^4 \ln \frac{m_{\hat{d}_+}^2}{\Lambda^2} + 2m_{\hat{d}_-}^4 \ln \frac{m_{\hat{d}_-}^2}{\Lambda^2} \right. \\ &\quad \left. - 4m_{\hat{\psi}_{\bar{g}d}}^4 \ln \frac{m_{\hat{\psi}_{\bar{g}d}}^2}{\Lambda^2} - 4m_{\hat{\psi}_{g\bar{d}}}^4 \ln \frac{m_{\hat{\psi}_{g\bar{d}}}^2}{\Lambda^2} \right). \end{aligned} \quad (3.14c)$$

Here Λ is a renormalization mass scale. Based on the action of Eq. (3.12) with $\widehat{V}_{\text{HI}} \simeq \widehat{V}_{\text{HI0}} + V_{\text{rc}}$, we can proceed to the analysis of non-MHI in the EF, employing the standard slow-roll approximation [45,46]. It can be shown [47] that the results calculated this way are the same as if we had calculated them using the non-minimally coupled scalar field in the JF.

3.2 THE INFLATIONARY OBSERVABLES – REQUIREMENTS

Under the assumption that there is a conventional cosmological evolution (see below) after non-MHI, the model parameters can be restricted, imposing the following requirements:

3.2.1 According to the inflationary paradigm, the horizon and flatness problems of the standard Big Bag cosmology can be successfully resolved provided that the number of e-foldings, \widehat{N}_* , that the scale $k_* = 0.002/\text{Mpc}$ suffers during non-MHI takes a certain value, which depends on the details of the cosmological model. The required \widehat{N}_* can be easily derived [23], consistently with our assumption of a conventional post-inflationary evolution. In particular, we assume that non-MHI is followed successively by the following three epochs: (i) the decaying-inflaton dominated era which lasts until the reheating temperature T_{rh} , (ii) a radiation dominated epoch, with initial temperature T_{rh} , which terminates at the matter-radiation equality, (iii) the matter dominated era until today. Employing standard methods [8,23], we can easily derive the required \widehat{N}_* for our model, with the result:

$$\widehat{N}_* \simeq 22.5 + 2 \ln \frac{V_{\text{HI}}(h_*)^{1/4}}{1 \text{ GeV}} - \frac{4}{3} \ln \frac{V_{\text{HI}}(h_f)^{1/4}}{1 \text{ GeV}} + \frac{1}{3} \ln \frac{T_{\text{rh}}}{1 \text{ GeV}} + \frac{1}{2} \ln \frac{f(h_f)}{f(h_*)}. \quad (3.15)$$

On the other hand, \widehat{N}_* can be calculated via the relation

$$\widehat{N}_* = \frac{1}{m_{\text{P}}^2} \int_{\widehat{h}_f}^{\widehat{h}_*} d\widehat{h} \frac{\widehat{V}_{\text{HI}}}{\widehat{V}_{\text{HI},\widehat{h}}} = \frac{1}{m_{\text{P}}^2} \int_{h_f}^{h_*} dh J^2 \frac{\widehat{V}_{\text{HI}}}{\widehat{V}_{\text{HI},h}}, \quad (3.16)$$

where $h_* [\widehat{h}_*]$ is the value of h [\widehat{h}] when k_* crosses the inflationary horizon. Also $h_f [\widehat{h}_f]$ is the value of h [\widehat{h}] at the end of non-MHI determined, in the slow-roll approximation, by the condition – see e.g. Ref. [45,46]:

$$\max\{\widehat{\epsilon}(h_f), |\widehat{\eta}(h_f)|\} = 1, \quad \text{where}$$

$$\hat{\epsilon} = \frac{m_{\text{P}}^2}{2} \left(\frac{\widehat{V}_{\text{HI},\hat{h}}}{\widehat{V}_{\text{HI}}} \right)^2 = \frac{m_{\text{P}}^2}{2J^2} \left(\frac{\widehat{V}_{\text{HI},h}}{\widehat{V}_{\text{HI}}} \right)^2 \simeq \frac{4m_{\text{P}}^4 (1 + 4c_{\mathcal{R}}m_{\text{PS}}^2)^2}{3c_{\mathcal{R}}^2 h^4} \quad (3.17a)$$

$$\text{and} \quad \hat{\eta} = m_{\text{P}}^2 \frac{\widehat{V}_{\text{HI},\hat{h}\hat{h}}}{\widehat{V}_{\text{HI}}} = \frac{m_{\text{P}}^2}{J^2} \left(\frac{\widehat{V}_{\text{HI},hh}}{\widehat{V}_{\text{HI}}} - \frac{\widehat{V}_{\text{HI},h}}{\widehat{V}_{\text{HI}}} \frac{J,h}{J} \right) \simeq -\frac{4m_{\text{P}}^2 (1 + 4c_{\mathcal{R}}m_{\text{PS}}^2)}{3c_{\mathcal{R}}h^2}, \quad (3.17b)$$

are the slow-roll parameters. Here we employ Eq. (3.6) and the following approximate relations:

$$J \simeq \sqrt{6} \frac{m_{\text{P}}}{h}, \quad \widehat{V}_{\text{HI},h} \simeq \frac{4\widehat{V}_{\text{HI}}}{c_{\mathcal{R}}h^3} m_{\text{P}}^2 (1 + 4c_{\mathcal{R}}m_{\text{PS}}^2) \quad \text{and} \quad \widehat{V}_{\text{HI},hh} \simeq -\frac{12\widehat{V}_{\text{HI}}}{c_{\mathcal{R}}h^4} m_{\text{P}}^2 (1 + 4c_{\mathcal{R}}m_{\text{PS}}^2). \quad (3.18)$$

The numerical computation reveals that non-MHI terminates due to the violation of the $\hat{\epsilon}$ criterion at a value of h equal to h_{f} , which is calculated to be

$$\hat{\epsilon}(h_{\text{f}}) = 1 \Rightarrow h_{\text{f}} = (4/3)^{1/4} m_{\text{P}} \sqrt{(1 + 4c_{\mathcal{R}}m_{\text{PS}}^2) / c_{\mathcal{R}}}. \quad (3.19)$$

Given that $h_{\text{f}} \ll h_*$, we can write h_* as a function of \widehat{N}_* as follows

$$\widehat{N}_* \simeq \frac{3c_{\mathcal{R}}}{4} \frac{h_*^2 - h_{\text{f}}^2}{(1 + 4c_{\mathcal{R}}m_{\text{PS}}^2)m_{\text{P}}^2} \Rightarrow h_* = 2m_{\text{P}} \sqrt{\widehat{N}_* (1 + 4c_{\mathcal{R}}m_{\text{PS}}^2) / 3c_{\mathcal{R}}}. \quad (3.20)$$

3.2.2 The power spectrum $P_{\mathcal{R}}$ of the curvature perturbations generated by h at the pivot scale k_* is to be confronted with the WMAP7 data [14], i.e.

$$P_{\mathcal{R}}^{1/2} = \frac{1}{2\sqrt{3}\pi m_{\text{P}}^3} \frac{\widehat{V}_{\text{HI}}(\hat{h}_*)^{3/2}}{|\widehat{V}_{\text{HI},\hat{h}}(\hat{h}_*)|} = \frac{1}{2\pi m_{\text{P}}^2} \sqrt{\frac{\widehat{V}_{\text{HI}}(h_*)}{6\hat{\epsilon}(h_*)}} \simeq 4.93 \cdot 10^{-5}. \quad (3.21)$$

Note that since the scalars listed in Table 2 are massive enough during non-MHI, the curvature perturbations generated by h are solely responsible for $P_{\mathcal{R}}$. Substituting Eqs. (3.17a) and (3.20) into the relation above, we obtain

$$P_{\mathcal{R}}^{1/2} \simeq \frac{\lambda h_*^2}{16\sqrt{2}\pi m_{\text{P}}^2 (1 + 4c_{\mathcal{R}}m_{\text{PS}}^2)} \simeq \frac{\lambda \widehat{N}_*}{12\sqrt{2}\pi c_{\mathcal{R}}}. \quad (3.22)$$

Combining the last equality with Eq. (3.21), we find that λ is to be proportional to $c_{\mathcal{R}}$, for almost constant \widehat{N}_* . Indeed, we obtain

$$\lambda \simeq 8.4 \cdot 10^{-4} \pi c_{\mathcal{R}} / \widehat{N}_* \Rightarrow c_{\mathcal{R}} \simeq 20925\lambda \quad \text{for} \quad \widehat{N}_* \simeq 55. \quad (3.23)$$

3.2.3 The (scalar) spectral index n_{s} , its running a_{s} , and the scalar-to-tensor ratio r must be consistent with the fitting [14] of the WMAP7, BAO and H_0 data, i.e.,

$$\text{(a) } n_{\text{s}} = 0.968 \pm 0.024, \quad \text{(b) } -0.062 \leq a_{\text{s}} \leq 0.018 \quad \text{and} \quad \text{(c) } r < 0.24 \quad (3.24)$$

at 95% confidence level (c.l.). The observable quantities above can be estimated through the relations:

$$n_{\text{s}} = 1 - 6\hat{\epsilon}_* + 2\hat{\eta}_* \simeq 1 - 2/\widehat{N}_*, \quad (3.25a)$$

$$\alpha_{\text{s}} = \frac{2}{3} (4\hat{\eta}_*^2 - (n_{\text{s}} - 1)^2) - 2\hat{\xi}_* \simeq -2\hat{\xi}_* \simeq -2/\widehat{N}_*^2 \quad (3.25b)$$

$$\text{and} \quad r = 16\hat{\epsilon}_* \simeq 12/\widehat{N}_*^2, \quad (3.25c)$$

where $\hat{\xi} = m_{\text{P}}^4 \widehat{V}_{\text{HI},h} \widehat{V}_{\text{HI},h\hat{h}\hat{h}} / \widehat{V}_{\text{HI}}^2 = m_{\text{P}} \sqrt{2\hat{\epsilon}} \hat{\eta}_h / J + 2\hat{\eta}\hat{\epsilon}$. The variables with subscript $*$ are evaluated at $h = h_*$ and Eqs. (3.17a) and (3.17b) have been employed.

3.2.4 The scale M_{PS} can be determined by requiring that the v.e.vs of the Higgs fields take the values dictated by the unification of the gauge couplings within the MSSM. Since the highest mass scale of the model – see Table 2 – in the SUSY vacuum, Eq. (2.16), is

$$m_{\perp 0} = \sqrt{5/2} f_0 g |\langle \nu_H^c \rangle| \quad \text{with} \quad f_0 = f(\langle h \rangle) = 1 + 4c_{\mathcal{R}} m_{\text{PS}}^2 \quad (3.26)$$

(recall that $m_{\text{PS}} = M_{\text{PS}}/m_{\text{P}}$) we can identify it with the unification scale M_{GUT} , i.e.

$$m_{\perp} = \sqrt{\frac{5}{2}} \frac{g M_{\text{PS}}}{f_0} = M_{\text{GUT}} \Rightarrow M_{\text{PS}} = \frac{\sqrt{2} M_{\text{GUT}} m_{\text{P}}}{(5g^2 m_{\text{P}}^2 - 2c_{\mathcal{R}} M_{\text{GUT}}^2)^{1/2}} \quad (3.27)$$

The requirement $5g^2 m_{\text{P}}^2 > 2c_{\mathcal{R}} M_{\text{GUT}}^2$ sets an upper bound on $c_{\mathcal{R}}$, which however can be significantly lowered if we impose the requirement of Sec. 3.2.1 – see below. When $c_{\mathcal{R}}$ ranges within its allowed region, we take $M_{\text{PS}} \simeq (1.81 - 2.2) \cdot 10^{16}$ GeV.

3.2.5 For the realization of non-MHI, we assume that $c_{\mathcal{R}}$ takes relatively large values – see e.g. Eq. (3.8). This assumption may [2, 48] jeopardize the validity of the classical approximation, on which the analysis of the inflationary behavior is based. To avoid this inconsistency – which is rather questionable [10, 48] though – we have to check the hierarchy between the ultraviolet cut-off, $\Lambda = m_{\text{P}}/c_{\mathcal{R}}$, of the effective theory and the inflationary scale, which is represented by $\widehat{V}_{\text{HI}}(h_*)^{1/4}$ or, less restrictively, by the corresponding Hubble parameter, $\widehat{H}_* = \widehat{V}_{\text{HI}}(h_*)^{1/2}/\sqrt{3}m_{\text{P}}$. In particular, the validity of the effective theory implies [48]

$$(a) \widehat{V}_{\text{HI}}(h_*)^{1/4} \leq \Lambda \quad \text{or} \quad (b) \widehat{H}_* \leq \Lambda \quad \text{for} \quad (c) \quad c_{\mathcal{R}} \geq 1. \quad (3.28)$$

3.3 NUMERICAL RESULTS

As can be easily seen from the relevant expressions above, the inflationary dynamics of our model depends on the following parameters:

$$\lambda, \lambda_H, \lambda_{\bar{H}}, k_S, c_{\mathcal{R}} \quad \text{and} \quad T_{\text{rh}}.$$

Recall that we determine M_{PS} via Eq. (3.27) with $g = 0.7$. Our results are essentially independent of λ_H , $\lambda_{\bar{H}}$ and k_S , provided that we choose some relatively large values for these so as $m_{\hat{u}_-}^2$, $m_{\hat{d}_-}^2$ and $m_{\hat{S}}^2$ in Table 2 are positive for $\lambda < 1$. We therefore set $\lambda_H = \lambda_{\bar{H}} = 0.5$ and $k_S = 1$ throughout our calculation. Finally T_{rh} can be calculated self-consistently in our model as a function of the inflaton mass, m_{I} and the mass $M_{\text{I}\hat{\nu}^c}$ of the RH neutrino into which inflaton decays, and the unified Yukawa coupling constant y_{33} – see Sec. 4.1. However the inflationary predictions depend very weakly on T_{rh} , because T_{rh} appears in Eq. (3.15) through the one third of its logarithm, and consequently its variation upon some orders of magnitude has a minor impact on the required value of \widehat{N}_* , which remains almost constant and close to 55.

In our numerical code, we use as input parameters h_* , $M_{\text{I}\hat{\nu}^c}$ and $c_{\mathcal{R}}$. For every chosen $c_{\mathcal{R}} \geq 1$ and $M_{\text{I}\hat{\nu}^c}$, we restrict λ and h_* so that the conditions Eq. (3.15) and (3.21) are satisfied. In our numerical calculations, we use the complete formulas for the slow-roll parameters and $P_{\mathcal{R}}^{1/2}$ in Eqs. (3.17a), (3.17b) and (3.21) and not the approximate relations listed in Sec. 3.2 for the sake of presentation. Our results are displayed in Fig. 1, where we draw the allowed values of $c_{\mathcal{R}}$ (solid line), T_{rh} (dashed line) and the inflaton mass at the SUSY vacuum – see Sec. 4.1 – m_{I} (dot-dashed line) [h_{f} (solid line) and h_* (dashed line)] versus λ (a) [(b)] for $M_{\text{I}\hat{\nu}^c} = 10^{11}$ GeV. Note that the decay of the inflaton into a RH neutrino with the mass above is kinematically permitted, for the depicted λ 's. The lower bound of the depicted lines comes from the saturation of the Eq. (3.28c). The constraint of Eq. (3.28b) is satisfied along the various curves whereas Eq. (3.28a) is valid only along the gray and light gray segments of

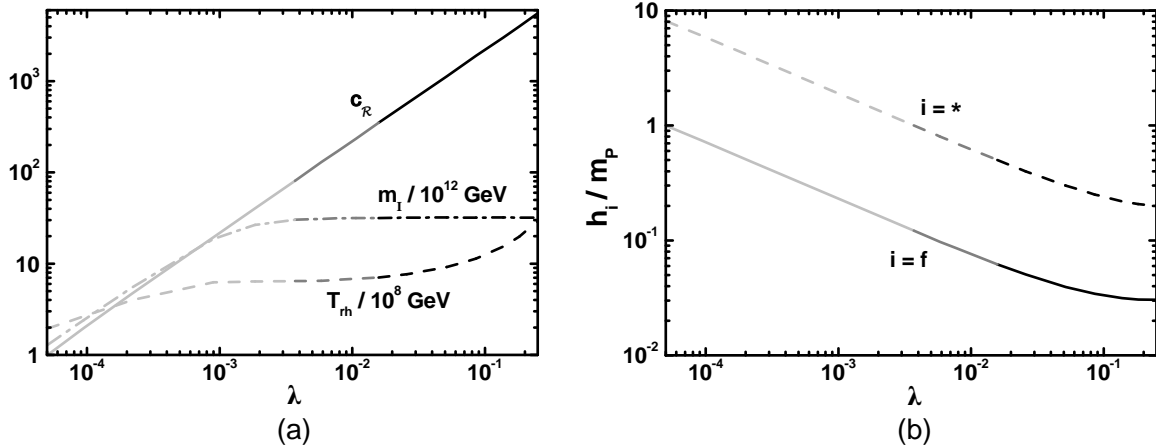


Figure 1: The allowed by Eqs. (3.15), (3.21), (3.28b) and (3.28c) values of $c_{\mathcal{R}}$ (solid line), T_{rh} – given by Eq. (4.7) – (dashed line) and m_{I} (dot-dashed line) [h_{f} (solid line) and h_{*} (dashed line)] versus λ (a) [(b)] for $k_S = 1$, $\lambda_H = \lambda_{\bar{H}} = 0.5$, $M_{\text{I}\bar{\nu}c} = 10^{11}$ GeV and $y_{33} = 0.5$. The light gray and gray segments denote values of the various quantities satisfying Eq. (3.28a) too, whereas along the light gray segments we obtain $h_{*} \geq m_{\text{P}}$.

these. Along the light gray segments, though, we obtain $h_{*} \geq m_{\text{P}}$. The latter regions of parameter space are not necessarily excluded [49], since the energy density of the inflaton remains sub-Planckian and so, corrections from quantum gravity can still be assumed to be small. As $c_{\mathcal{R}}$ increases beyond $5.6 \cdot 10^3$, $4c_{\mathcal{R}}m_{\text{PS}}$ becomes larger than 1, \hat{N}_{*} derived by Eq. (3.20) starts decreasing and therefore, non-MHI fails to fulfil the relevant requirement. All in all, we obtain

$$1 \lesssim c_{\mathcal{R}} \lesssim 5.6 \cdot 10^3 \quad \text{and} \quad 5 \cdot 10^{-5} \lesssim \lambda \lesssim 0.25 \quad \text{for} \quad 53.9 \lesssim \hat{N}_{*} \lesssim 55. \quad (3.29)$$

From Fig. 1-(a), we can verify our analytical estimation in Eq. (3.23) according to which λ is proportional to $c_{\mathcal{R}}$. On the other hand, the variation of h_{f} and h_{*} as a function of $c_{\mathcal{R}}$ – drawn in Fig. 1-(b) – is consistent with Eqs. (3.19) and (3.20). Note that the inclusion of the term $4c_{\mathcal{R}}M_{\text{PS}}^2$ in the numerators of these relations is crucial in order to obtain a reliable result for $\lambda \gtrsim 0.13$ or $c_{\mathcal{R}} \gtrsim 3 \cdot 10^3$ – cf. Ref. [11]. Letting λ or $c_{\mathcal{R}}$ vary within its allowed region in Eq. (3.29), we obtain

$$0.964 \lesssim n_{\text{s}} \lesssim 0.965, \quad -6.5 \lesssim \frac{\alpha_{\text{s}}}{10^{-4}} \lesssim -6.2 \quad \text{and} \quad 4.2 \gtrsim \frac{r}{10^{-3}} \gtrsim 3.5. \quad (3.30)$$

Clearly, the predicted α_{s} and r lie within the allowed ranges given in Eq. (3.24b) and Eq. (3.24c) respectively, whereas n_{s} turns out to be impressively close to its central observationally favored value – see Eq. (3.24a) and cf. Ref. [10].

4 NON-THERMAL LEPTOGENESIS

In this section, we specify how the SUSY inflationary scenario makes a transition to the radiation dominated era, and give an explanation of the origin of the observed BAU consistently with the \tilde{G} constraint. The main features of the post-inflationary evolution of our model are described in Sec. 4.1. In Sec. 4.2 we describe the additional constraints that we impose on our setting, and finally we delineate the allowed parameter space of our cosmological model in Sec. 4.3.

EIGENSTATES	MASSES	EIGENSTATES	MASSES
THE $S - \nu_H^c - \bar{\nu}_H^c$ SECTOR		THE $u_{Ha}^c - \bar{u}_{Ha}^c$ AND $e_H^c - \bar{e}_H^c$ SECTORS	
$\widehat{\delta h}$	$m_I = \sqrt{2}\lambda M_{\text{PS}}/\langle J \rangle f_0$	$\widehat{u}_{1-}^a, \widehat{u}_{2+}^a, \widehat{e}_{1-}, \widehat{e}_{2+}$	$gM_{\text{PS}}/\sqrt{f_0}$
$\widehat{\theta}_\nu$	$\sqrt{5/2}f_0 gM_{\text{PS}}$	$A_C^{a\pm}, A_R^\pm$	$gM_{\text{PS}}/\sqrt{f_0}$
$\widehat{\theta}_+$	$\sqrt{2}\lambda M_{\text{PS}}/J_0 f_0$	$\lambda_C^{a\pm}, \psi_u^a, \psi_{\bar{u}}^a$	$gM_{\text{PS}}/\sqrt{f_0}$
\widehat{S}	$\sqrt{2}\lambda M_{\text{PS}}/\sqrt{f_0}$	$\lambda_R^\pm, \psi_e, \psi_{\bar{e}}$	$gM_{\text{PS}}/\sqrt{f_0}$
A^\perp, A^\parallel	$\sqrt{5/2}f_0 gM_{\text{PS}}$	THE $d_{Ha}^c - \bar{d}_{Ha}^c$ AND $g_a^c - \bar{g}_a^c$ SECTORS	
A^\parallel	0	$\widehat{g}_1^a, \widehat{g}_2^a$	$2\lambda_H M_{\text{PS}}/\sqrt{f_0}$
$\widehat{\psi}_{S\nu\pm}$	$\sqrt{2}\lambda M_{\text{PS}}/\sqrt{f_0}$	$\widehat{g}_1^a, \widehat{g}_2^a$	$2\lambda_{\bar{H}} M_{\text{PS}}/\sqrt{f_0}$
$\lambda^\perp, \widehat{\psi}_{\nu-}$	$\sqrt{5/2}f_0 gM_{\text{PS}}$	$\widehat{d}_1^a, \widehat{d}_2^a$	$2\lambda_H M_{\text{PS}}/\sqrt{f_0}$
$\lambda^\parallel, \widehat{\psi}_{\nu+}$	0	$\widehat{d}_1^a, \widehat{d}_2^a$	$2\lambda_{\bar{H}} M_{\text{PS}}/\sqrt{f_0}$
THE ν_i^c SECTOR		$\widehat{\psi}_{gd\pm}^a$	$2\lambda_H M_{\text{PS}}/\sqrt{f_0}$
$\widehat{\nu}_i^c, \widehat{\bar{\nu}}_i^c$	$M_{i\widehat{\nu}^c} = 2\lambda_{i\nu^c} M_{\text{PS}}^2/M_S\sqrt{f_0}$	$\widehat{\psi}_{g\bar{d}\pm}^a$	$2\lambda_{\bar{H}} M_{\text{PS}}/\sqrt{f_0}$

Table 3: The mass spectrum of our model at the SUSY vacuum of Eq. (2.16). We use the abbreviations $\langle J \rangle = J(h = 2M_{\text{PS}})$, $f_0 = 1 + 4c_{\mathcal{R}}m_{\text{PS}}^2$ and $\bar{f}_0 = f_0 + 24c_{\mathcal{R}}^2 m_{\text{PS}}^2 \simeq J_0^2$. The various eigenstates and symbols are specified in Sec. 3.1 and Appendix A.

4.1 THE GENERAL SET-UP

When non-MHI is over, the inflaton continues to roll down towards the SUSY vacuum, Eq. (2.16). There is a brief stage of tachyonic preheating [51] which does not lead to significant particle production [52]. Soon after, as discussed in the Appendix B, the inflaton settles into a phase of damped oscillations initially around zero – where \widehat{V}_{HIO} has a maximum – and then around one of the minima of \widehat{V}_{HIO} . Whenever the inflaton passes through zero, particle production may occur creating mostly superheavy bosons via the mechanism of instant preheating [53]. This process becomes more efficient as λ decreases, and further numerical investigation is required in order to check the viability of our leptogenesis scenario detailed below. For this reason, we restrict to λ 's larger than 0.001, which ensures a less frequent passage of the inflaton through zero, weakening thereby the effects from instant preheating and other parametric resonance effects – see Appendix B. Intuitively the reason is that larger λ 's require larger $c_{\mathcal{R}}$'s, see Eq. (3.23), diminishing therefore h_f given by Eq. (3.20), which sets the amplitude of the very first oscillations.

Nonetheless the standard perturbative approach to the inflaton decay provides a very efficient decay rate. This is to be contrasted with the SM (or next-to-MSSM) non-MHI, where the consideration of non-perturbative effects is imperative [52] in order to obtain successful reheating. Namely, at the SUSY vacuum ν_H^c and $\bar{\nu}_H^c$ acquire the v.e.vs shown in Eq. (2.16) giving rise to the mass spectrum presented in Table 3. Note that the masses of the various scalars – contrary to the masses of the fermions and gauge bosons – are not derived from the corresponding formulas listed in Table 2 with the naive replacement $x_h = 2m_{\text{PS}}$, since terms proportional to m_{PS}^2 are neglected there. In Table 3 we also show the mass, m_I , of the (canonically normalized) inflaton $\widehat{\delta h} = (h - 2M_{\text{PS}})/J_0$ and the masses $M_{i\widehat{\nu}^c}$ of the RH neutrinos, ν_i^c , which play a crucial role in our leptogenesis scenario – we assume the existence of a term similar to the second one inside \ln of Eq. (2.12) for ν_i^c too. From Fig. 1 we notice that m_I increases with λ – as in the case of HI, cf. Ref. [19] – only for $\lambda \lesssim 0.0013$ or $c_{\mathcal{R}} \leq 30$. For larger λ 's

$\langle J \rangle = J(h = 2M_{\text{PS}})$ ranges from 3 to 90 and so m_{I} is kept independent of λ and almost constant at the level of 10^{13} GeV. Indeed, if we express $\widehat{\delta h}$ as a function of δh through the relation

$$\frac{\widehat{\delta h}}{\delta h} \simeq J_0 \quad \text{where} \quad J_0 = \sqrt{1 + \frac{3}{2}m_{\text{P}}^2 f_{,h}^2(\langle h \rangle)} = \sqrt{1 + 24c_{\mathcal{R}}^2 m_{\text{PS}}^2} \quad (4.1)$$

is obtained by expanding J given in Eq. (3.11) at leading order in x_h , we find

$$m_{\text{I}} \simeq \frac{\sqrt{2}\lambda M_{\text{PS}}}{f_0 J_0} \simeq \frac{\lambda m_{\text{P}}}{2\sqrt{3}c_{\mathcal{R}}} \simeq \frac{10^{-4}m_{\text{P}}}{4.2\sqrt{3}} \simeq 3 \cdot 10^{13} \text{ GeV} \quad \text{for} \quad \lambda \gtrsim \frac{10^{-4}}{4.2\sqrt{6}m_{\text{PS}}} \simeq 1.3 \cdot 10^{-3} \quad (4.2)$$

where we make use of Eq. (3.23) – note that $f_0 \simeq 1$. Apart from some fields in the ν_i^c sector, $\widehat{\delta h}$ is the lightest among the massive particles listed in Table 3 for λ given in Eq. (3.29), since $\langle J \rangle \gg 1$ and g, λ_H and $\lambda_{\bar{H}}$ are taken larger than λ . Therefore perturbative decays of $\widehat{\delta h}$ into these massive particles are kinematically forbidden. For the same reason narrow parametric resonance [51] effects are absent. Also $\widehat{\delta h}$ can not decay via renormalizable interaction terms to SM particles.

The various decay channels of the inflaton are mainly determined by the Lagrangian part containing two fermions – see Eq. (A.15). The inflaton can decay into a pair of RH neutrinos ($\widehat{\nu}_i^c$) through the following lagrangian terms:

$$\mathcal{L}_{\text{I}\nu_i^c} = -\lambda_{i\nu^c} \frac{M_{\text{PS}} f_0}{M_{\text{S}}} (1 - 12c_{\mathcal{R}} m_{\text{PS}}^2) \widehat{\delta h} \widehat{\nu}_i^c \widehat{\nu}_i^c + \text{h.c.} \quad (4.3)$$

From Eq. (4.3) we deduce that the decay of $\widehat{\delta h}$ into $\widehat{\nu}_i^c$ is induced by two lagrangian terms. The first one originates exclusively from the non-renormalizable term of Eq. (2.9) – as in the case of a similar model in Ref. [19]. The second term is a higher order decay channel due to the SUGRA lagrangian – cf. Ref. [54]. The interaction in Eq. (4.3) gives rise to the following decay width

$$\Gamma_{\text{I}\nu^c} = \frac{c_{\text{I}\nu^c}^2}{64\pi} m_{\text{I}} \sqrt{1 - \frac{4M_{\text{I}\widehat{\nu}^c}^2}{m_{\text{I}}^2}} \quad \text{with} \quad c_{\text{I}\nu^c} = \frac{M_{\text{I}\widehat{\nu}^c} f_0^{3/2}}{M_{\text{PS}} J_0} (1 - 12c_{\mathcal{R}} m_{\text{PS}}^2), \quad (4.4)$$

where $M_{\text{I}\widehat{\nu}^c}$ is the Majorana mass of the RH neutrino into which the inflaton can decay – see Table 3. In addition, it was [54] recently recognized that within SUGRA the inflaton can decay to the MSSM particles spontaneously – i.e., even without direct superpotential couplings – via non renormalizable interaction terms. For a typical trilinear superpotential term of the form $W_y = yXYZ$, we obtain the effective interactions described by the langrangian part

$$\mathcal{L}_{\text{I}y} = 6yc_{\mathcal{R}} \frac{M_{\text{PS}} f_0^{3/2}}{m_{\text{P}}^2} \widehat{\delta h} \left(\widehat{X} \widehat{\psi}_Y \widehat{\psi}_Z + \widehat{Y} \widehat{\psi}_X \widehat{\psi}_Z + \widehat{Z} \widehat{\psi}_X \widehat{\psi}_Y \right) + \text{h.c.}, \quad (4.5)$$

where y is a Yukawa coupling constant, ψ_X, ψ_Y and ψ_Z are the chiral fermions associated with the superfields X, Y and Z , and whose scalar components are denoted with the superfield symbol. For these scalars a term similar to the second one inside ln of Eq. (2.12) is assumed so as to obtain canonically normalized scalars and spinors through relations similar to the last equalities in Eqs. (3.11) and (A.14) respectively. Taking into account the terms of Eq. (2.6) and the fact that the adopted SUSY GUT predicts Yukawa unification for the 3rd generation at M_{PS} , we conclude that the interaction above gives rise to the following 3-body decay width

$$\Gamma_{\text{I}y} = \frac{14c_{\text{I}y}^2}{512\pi^3} m_{\text{I}}^3 \simeq \frac{3y_{33}^2}{64\pi^3} f_0^3 \left(\frac{m_{\text{I}}}{m_{\text{P}}} \right)^2 m_{\text{I}} \quad \text{where} \quad c_{\text{I}y} = 6y_{33}c_{\mathcal{R}} \frac{M_{\text{PS}} f_0^{3/2}}{m_{\text{P}}^2 J_0}, \quad (4.6)$$

with $y_{33} \simeq (0.4 - 0.6)$ being the common Yukawa coupling constant of the third generation computed at the m_I scale and summation is taken over color and weak hypercharge d.o.f, in conjunction with the assumption that $m_I < 2M_{3\widehat{\nu}^c}$ which is valid for both inflaton-decay scenaria considered below.

Since the decay width of the produced $\widehat{\nu}_1^c$ is much larger than Γ_I – see below – the reheating temperature, T_{rh} , is exclusively determined by the inflaton decay and is given by [55]

$$T_{\text{rh}} = \left(\frac{72}{5\pi^2 g_*} \right)^{1/4} \sqrt{\Gamma_I m_{\text{P}}} \quad \text{with} \quad \Gamma_I = \Gamma_{\text{I}\nu^c} + \Gamma_{\text{I}y}, \quad (4.7)$$

where g_* counts the effective number of relativistic degrees of freedom at temperature T_{rh} . For the MSSM spectrum, $g_* \simeq 228.75$. From Fig. 1 we remark that T_{rh} does not exclusively increase with λ , but rather follows the behavior of m_I . For $M_{\text{I}\widehat{\nu}^c} = 10^{11}$ GeV, we find that $\Gamma_{\text{I}y}$ dominates over $\Gamma_{\text{I}\nu^c}$ for $\lambda \gtrsim 0.002$ or – via Eq. (3.23) – $c_{\mathcal{R}} \geq 50$. For $0.0013 \lesssim \lambda \lesssim 0.03$, T_{rh} remains almost constant since $f_0^3 \simeq 1$ – see Eq. (4.6). For $\lambda \gtrsim 0.03$, $f_0^3 \simeq 1 + 12c_{\mathcal{R}}m_{\text{PS}}^2$ starts to deviate from unity and so, T_{rh} increases as shown in Fig. 1.

If $T_{\text{rh}} < M_{\text{I}\widehat{\nu}^c}$, the out-of-equilibrium condition [31] for the implementation of leptogenesis is automatically satisfied. Subsequently $\widehat{\nu}_1^c$ decay into H_u and L_i^* via the tree-level couplings derived from the second term in the RHS of Eq. (2.6). Interference between tree-level and one-loop diagrams generates a lepton-number asymmetry ε_L [31], when CP conservation is violated. The resulting lepton-number asymmetry after reheating can be partially converted through sphaleron effects into baryon-number asymmetry. However, the required T_{rh} must be compatible with constraints for the \widetilde{G} abundance, $Y_{\widetilde{G}}$, at the onset of *nucleosynthesis* (BBN). In particular, the B yield can be computed as

$$(a) \ Y_B = -0.35Y_L \quad \text{with} \quad (b) \ Y_L = 2\varepsilon_L \frac{5}{4} \frac{\Gamma_{\text{I}\nu^c}}{\Gamma_I} \frac{T_{\text{rh}}}{m_I}. \quad (4.8)$$

The numerical factor in the RHS of Eq. (4.8a) comes from the sphaleron effects, whereas the numerical factor (5/4) in the RHS of Eq. (4.8b) is due to the slightly different calculation [55] of T_{rh} – cf. Ref. [31]. In the major part of our allowed parameter space – see Sec. 4.3 – $\Gamma_I \simeq \Gamma_{\text{I}y}$ and so the involved branching ratio of the produced $\widehat{\nu}_i^c$ is given by

$$\frac{\Gamma_{\text{I}\nu^c}}{\Gamma_I} \simeq \frac{\Gamma_{\text{I}\nu^c}}{\Gamma_{\text{I}y}} = \frac{\pi^2 (1 - 12c_{\mathcal{R}}m_{\text{PS}}^2)^2}{72c_{\mathcal{R}}^2 y_{33}^2 m_{\text{PS}}^4} \frac{M_{\text{I}\widehat{\nu}^c}^2}{m_I^2}. \quad (4.9)$$

For $M_{\text{I}\widehat{\nu}^c} \simeq (10^{11} - 10^{13})$ GeV the ratio above takes adequately large values so that Y_L is sizable. Therefore, the presence of more than one inflaton decay channels does not invalidate the non-thermal leptogenesis scenario. On the other hand, the \widetilde{G} yield at the onset of BBN is estimated to be [35]:

$$Y_{\widetilde{G}} \simeq c_{\widetilde{G}} T_{\text{rh}} \quad \text{with} \quad c_{\widetilde{G}} = 1.9 \cdot 10^{-22} / \text{GeV}. \quad (4.10)$$

Let us note that non-thermal \widetilde{G} production within SUGRA is [54] also possible. However, we here prefer to adopt the conservative approach based on the estimation of $Y_{\widetilde{G}}$ via Eq. (4.10) since the latter \widetilde{G} production depends on the mechanism of the SUSY breaking.

Both Eqs. (4.8) and (4.10) calculate the correct values of the B and \widetilde{G} abundances provided that no entropy production occurs for $T < T_{\text{rh}}$, as we already assumed – see Sec. 3.2. Regarding the estimation of ε_L , appearing in Eq. (4.8), we single out two cases below, according to whether the inflaton can decay into the lightest ($\widehat{\nu}_1^c$) or to the next-to-lightest ($\widehat{\nu}_2^c$) RH neutrino. Note that the decay of the inflaton to the heaviest RH neutrino ($\widehat{\nu}_3^c$) is disfavored by the kinematics and the \widetilde{G} constraint.

4.1.1 DECAY OF THE INFLATON TO THE LIGHTEST RH NEUTRINO

In this case, we suppose that the Majorana masses of ν_i^c are hierarchical, with $M_{1\hat{\nu}^c} \ll M_{2\hat{\nu}^c}, M_{3\hat{\nu}^c}$ (but with $M_{1\hat{\nu}^c} > T_{\text{rh}}$). The produced lepton-number asymmetry for a normal hierarchical mass spectrum of light neutrinos reads [31]

$$\varepsilon_L = -\frac{3}{8\pi} \frac{m_{\nu_\tau} M_{1\hat{\nu}^c}}{\langle H_u \rangle^2} \delta_{\text{eff}}. \quad (4.11)$$

Here $|\delta_{\text{eff}}| \leq 1$, which we treat as a free parameter, represents the magnitude of CP violation; m_{ν_τ} is the mass of heaviest light neutrino ν_τ and we take $\langle H_u \rangle = 174 \text{ GeV}$ – adopting the large $\tan \beta$ regime.

4.1.2 DECAY OF THE INFLATON TO THE NEXT-TO-LIGHTEST RH NEUTRINO

In this case, we assume $M_{1\hat{\nu}^c} \ll M_{2\hat{\nu}^c} \ll M_{3\hat{\nu}^c}$ and impose the conditions $T_{\text{rh}} < M_{2\hat{\nu}^c} < m_1/2$ and $M_{1\hat{\nu}^c} > T_{\text{rh}}$. The resulting lepton asymmetry is [19, 32]:

$$\varepsilon_L = \frac{3}{8\pi} \frac{M_{2\hat{\nu}^c}}{M_{3\hat{\nu}^c}} \frac{(m_{3\text{D}}^2 - m_{2\text{D}}^2)^2 s_\vartheta^2 c_\vartheta^2 \sin 2\delta}{\langle H_u \rangle^2 (m_{3\text{D}}^2 s_\vartheta^2 + m_{2\text{D}}^2 c_\vartheta^2)}, \quad (4.12)$$

where $m_{i\text{D}}$ are the Dirac masses of ν_i – in a basis where they are diagonal and positive – $c_\vartheta = \cos \vartheta$, $s_\vartheta = \sin \vartheta$, with ϑ and δ being the rotation angle and phase which diagonalize the Majorana-mass matrix, $M_{\hat{\nu}^c}$, of $\hat{\nu}^c$. The values of the various parameters are estimated at the leptogenesis scale. Note that since $M_{1\hat{\nu}^c} > T_{\text{rh}}$, ε_L calculated by Eq. (4.12) is not washed out due to $\hat{\nu}_1^c$ inverse decays and $\Delta L = 1$ scatterings – the case with $M_{1\hat{\nu}^c} < T_{\text{rh}}$ is treated in Ref. [56]. Also Eq. (4.12) holds provided that $M_{2\hat{\nu}^c} \ll M_{3\hat{\nu}^c}$ and the decay width of $\hat{\nu}_i^c$ is much smaller than $(M_{3\hat{\nu}^c}^2 - M_{2\hat{\nu}^c}^2)/M_{2\hat{\nu}^c}$. Both conditions are well satisfied here – see Sec. 4.3.2.

Since recent results [36] – see, also, Ref. [57] – show that the mixing angle θ_{13} can be taken (at 95% c.l.) equal to zero and earlier analysis [58] of the CHOOZ experiment [59] suggests that the solar and atmospheric neutrino oscillations decouple, we are allowed to concentrate on the two heaviest families ignoring the first one. This assumption enables us to connect this leptogenesis scenario with the oscillation parameters of the $\nu_\mu - \nu_\tau$ system. The light-neutrino mass matrix, m_ν , is given by the seesaw formula:

$$m_\nu = -m_{\text{D}}^{\text{T}} M_{\hat{\nu}^c}^{-1} m_{\text{D}}, \quad (4.13)$$

where m_{D} is the Dirac mass matrix of the ν_i . The determinant and the trace invariance of $m_\nu^\dagger m_\nu$ imply two constraints on the parameters involved, i.e.

$$m_{2\text{D}}^2 m_{3\text{D}}^2 = m_{\nu_\tau} m_{\nu_\mu} M_{2\hat{\nu}^c} M_{3\hat{\nu}^c} \quad \text{and} \quad A_{\text{D}} s_\vartheta^2 + B_{\text{D}} s_\vartheta + C_{\text{D}} = 0 \quad (4.14)$$

with the coefficient of the latter equation being

$$\begin{aligned} A_{\text{D}} &= (m_{2\text{D}}^2 - m_{3\text{D}}^2) \left((m_{2\text{D}}^2 - m_{3\text{D}}^2) M_{2\hat{\nu}^c}^2 + (m_{2\text{D}}^2 - m_{3\text{D}}^2) M_{3\hat{\nu}^c}^2 \right. \\ &\quad \left. + 2(m_{2\text{D}}^2 + m_{3\text{D}}^2) M_{2\hat{\nu}^c} M_{3\hat{\nu}^c} \cos 2\delta \right) \end{aligned} \quad (4.15a)$$

$$\begin{aligned} B_{\text{D}} &= 2(m_{2\text{D}}^2 - m_{3\text{D}}^2) \left(m_{3\text{D}}^2 M_{2\hat{\nu}^c}^2 - m_{2\text{D}}^2 M_{3\hat{\nu}^c}^2 \right. \\ &\quad \left. - (m_{2\text{D}}^2 + m_{3\text{D}}^2) M_{2\hat{\nu}^c} M_{3\hat{\nu}^c} \cos 2\delta \right) \end{aligned} \quad (4.15b)$$

$$C_{\text{D}} = (m_{2\text{D}}^4 M_{3\hat{\nu}^c}^2 + m_{3\text{D}}^4 M_{2\hat{\nu}^c}^2) - (m_{\nu_\tau}^2 + m_{\nu_\mu}^2) M_{2\hat{\nu}^c}^2 M_{3\hat{\nu}^c}^2. \quad (4.15c)$$

Assuming that the Dirac mixing angle (i.e., the mixing angle in the absence of RH neutrino Majorana masses) is negligible, we can identify [32] the rotation angle which diagonalizes m_ν with the physical mixing angle in the $\nu_\mu - \nu_\tau$ leptonic sector, θ_{23} , which is constrained by the present neutrino data – see below.

4.2 IMPOSED CONSTRAINTS

The parameters of our model can be further restricted if, in addition to the inflationary requirements mentioned in Sec. 3.2 and the restriction $\lambda \geq 0.001$ which allows us to ignore effects of instant preheating – see Appendix B – we impose extra constraints arising from the post-inflationary scenario. These are the following:

4.2.1 To ensure that the inflaton decay to RH neutrinos is kinematically allowed we have to impose the constraint:

$$m_{\text{I}} \geq 2M_{\text{I}\hat{\nu}^c} \Rightarrow M_{\text{I}\hat{\nu}^c} \lesssim \lambda m_{\text{P}}/4\sqrt{3}c_{\mathcal{R}} \simeq 1.5 \cdot 10^{13} \text{ GeV} \text{ for } \lambda \gtrsim 1.3 \cdot 10^{-3}, \quad (4.16)$$

where we make use of Eq. (4.2). More specifically, we require $m_{\text{I}} \geq 2M_{\text{I}\hat{\nu}^c}$ [$m_{\text{I}} \geq 2M_{2\hat{\nu}^c}$] for the scenario described in Sec. 4.1.1 [Sec. 4.1.2].

4.2.2 In agreement with our assumption about hierarchical light neutrino masses for both inflaton-decay scenaria, the solar and atmospheric neutrino mass squared differences Δm_{\odot}^2 and Δm_{\oplus}^2 can be identified with the squared masses of ν_{μ} and ν_{τ} , $m_{\nu_{\mu}}^2$ and $m_{\nu_{\tau}}^2$, respectively. Taking the central values of the former quantities [36], we set:

$$(a) \ m_{\nu_{\mu}} = \sqrt{\Delta m_{\odot}^2} = 0.0087 \text{ eV} \text{ and } (b) \ m_{\nu_{\tau}} = \sqrt{\Delta m_{\oplus}^2} = 0.05 \text{ eV}. \quad (4.17)$$

We multiply the values above by 1.12 in order to roughly approximate renormalization group effects for the evolution of these masses from the electroweak up to the leptogenesis scale – see Fig. 4 of Ref. [60]. The resulting $m_{\nu_{\tau}}(T_{\text{rh}})$ is low enough to ensure that the lepton asymmetry is not erased by lepton number violating $2 \rightarrow 2$ scatterings [61] at all temperatures between T_{rh} and 100 GeV. Also $\sin^2 \theta_{23}$ is to be consistent with the following 95% c.l. allowed range [36]:

$$0.41 \lesssim \sin^2 \theta_{23} \lesssim 0.61. \quad (4.18)$$

4.2.3 Due to the presence of $SU(4)_{\text{C}}$ symmetry in G_{PS} , $m_{3\text{D}}$ coincides with the value of the top quark mass, m_t , at the leptogenesis scale – see also Eq. (2.6) – i.e.

$$m_{3\text{D}}(T_{\text{rh}}) = m_t(T_{\text{rh}}). \quad (4.19)$$

Working in the context of the MSSM with $\tan \beta = 50$, and solving the relevant renormalization group equations, we find $m_t(T_{\text{rh}}) \simeq (120 - 126) \text{ GeV}$ for the values of T_{rh} encountered in our set-up.

4.2.4 The implementation of BAU via non-thermal leptogenesis dictates [14] at 95% c.l.

$$Y_B = (8.74 \pm 0.42) \cdot 10^{-11} \Rightarrow 8.32 \leq Y_B/10^{-11} \leq 9.16. \quad (4.20)$$

4.2.5 In order to avoid spoiling the success of the BBN, an upper bound on $Y_{\tilde{G}}$ is to be imposed depending on the \tilde{G} mass, $m_{\tilde{G}}$, and the dominant \tilde{G} decay mode. For the conservative case where \tilde{G} decays with a tiny hadronic branching ratio, we have [35]

$$Y_{\tilde{G}} \lesssim \begin{cases} 10^{-15} \\ 10^{-14} \\ 10^{-13} \\ 10^{-12} \end{cases} \text{ for } m_{\tilde{G}} \simeq \begin{cases} 0.45 \text{ TeV} \\ 0.69 \text{ TeV} \\ 10.6 \text{ TeV} \\ 13.5 \text{ TeV}. \end{cases} \quad (4.21)$$

The bound above can be somehow relaxed in the case of a stable \tilde{G} . As we see below, this bound is achievable within our model only for $m_{\tilde{G}} > 10 \text{ TeV}$. As $m_{\tilde{G}}$ gets larger than this bound leads to the necessity of a rather fine tuned SUSY breaking mechanism such as split SUSY [63], or anomaly mediated SUSY breaking [64] where the superpartners of SM particles have masses lower than $m_{\tilde{G}}$. Using Eq. (4.10) the bounds on $Y_{\tilde{G}}$ can be translated into bounds on T_{rh} . Specifically we take $T_{\text{rh}} \simeq (0.53 - 5.3) \cdot 10^8 \text{ GeV}$ [$T_{\text{rh}} \simeq (0.53 - 5.3) \cdot 10^9 \text{ GeV}$] for $Y_{\tilde{G}} \simeq (0.1 - 1) \cdot 10^{-13}$ [$Y_{\tilde{G}} \simeq (0.1 - 1) \cdot 10^{-12}$].

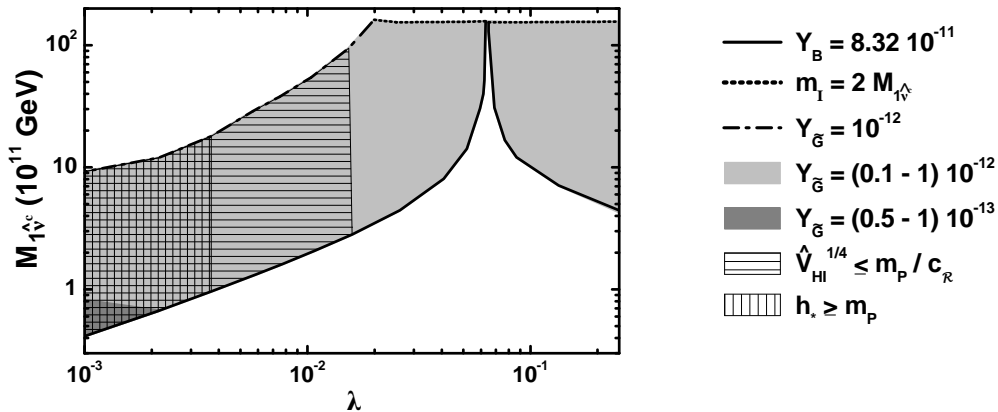


Figure 2: Allowed (shaded) regions in the $\lambda - M_{1\hat{\nu}^c}$ plane, for $\lambda_H = \lambda_{\bar{H}} = 0.5$, $k_S = 1$ and $y_{33} = 0.5$ when the inflaton can decay into $\hat{\nu}_1^c$'s. The conventions adopted for the various lines and shaded or hatched regions are also shown.

4.3 NUMERICAL RESULTS

Considering the constraints above in conjunction with those quoted in Sec. 3.2, we can delineate the overall allowed parameter space of our model. Recall that we set $\lambda_H = \lambda_{\bar{H}} = 0.5$, $k_S = 1$ and $g = 0.7$ with M_{PS} given by Eq. (3.27). The upper [lower] bound of the used λ 's comes from Eq. (3.29) [the conclusions of Appendix B]. Also we fix $y_{33} = 0.5$ throughout our investigation. As can be deduced by Eqs. (4.8) and (4.9), for lower [larger] y_{33} 's satisfying Eq. (4.20) requires slightly [lower] larger $M_{1\hat{\nu}^c}$'s. As mentioned in Sec. 4.1, we adopt two leptogenesis scenaria depending on whether $\delta\hat{h}$ can decay to $\hat{\nu}_1^c$ or $\hat{\nu}_2^c$. As we see below, in both cases, two disconnected allowed domains arise according to which of the two contributions in Eq. (4.3) dominates. The critical point $(\lambda_c, c_{\mathcal{R}c})$ is extracted from:

$$1 - 12c_{\mathcal{R}c}m_{\text{PS}}^2 = 0 \Rightarrow c_{\mathcal{R}c} = 1/12m_{\text{PS}}^2 \text{ or } \lambda_c \simeq 10^{-4}/25.2m_{\text{PS}}^2 \simeq 0.06 \quad (4.22)$$

where we make use of Eq. (3.23) in the last step. From Eqs. (4.7), (4.8) and (4.9) one can deduce that for $\lambda < \lambda_c$, T_{rh} remains almost constant; $\Gamma_{1\nu^c}/\Gamma_I$ decreases as $c_{\mathcal{R}}$ increases and so the $M_{1\hat{\nu}^c}$'s, which satisfy Eq. (4.20), increase. On the contrary, for $\lambda > \lambda_c$, $\Gamma_{1\nu^c}/\Gamma_I$ is independent of $c_{\mathcal{R}}$ but T_{rh} increases with $c_{\mathcal{R}}$ and so fulfilling Eq. (4.20) $M_{1\hat{\nu}^c}$'s decrease.

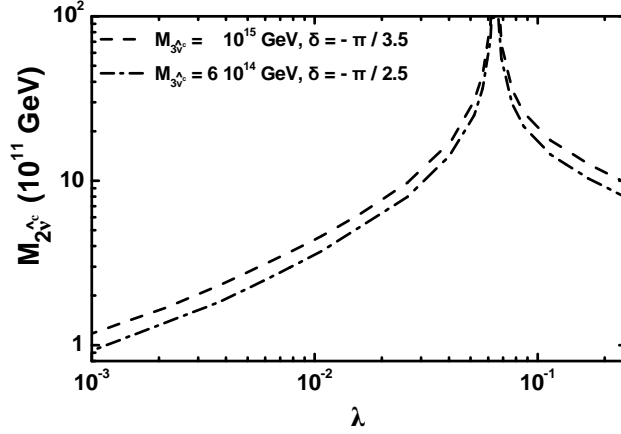
In the following, we present the results of our investigation in each case, separately.

4.3.1. Decay of the inflaton into $\hat{\nu}_1^c$. In this case our cosmological setting depends on the following parameters:

$$\lambda, c_{\mathcal{R}}, M_{1\hat{\nu}^c} \text{ and } \delta_{\text{eff}}.$$

Given our ignorance about δ_{eff} in Eq. (4.11), we take $\delta_{\text{eff}} = 1$, allowing us to obtain via Eq. (4.11) the maximal [62] possible $|\varepsilon_L|$. This choice in conjunction with the imposition of the lower bound on Y_B in Eq. (4.20) provides the most conservative restriction on our parameters.

As we explain in Sec. 3.3, $M_{1\hat{\nu}^c}$ does not crucially influence the inflationary observables. On the contrary, $M_{1\hat{\nu}^c}$ plays a key-role in simultaneously satisfying Eqs. (4.16), (4.20) and (4.21) – see Eqs. (4.8) and (4.10). For this reason we display in Fig. 2 the allowed regions by all the imposed constraints in the $\lambda - M_{1\hat{\nu}^c}$ plane. In the horizontally lined regions Eq. (3.28a) holds, whereas in the vertically hatched region we get $h_* \geq m_p$. The restrictions on the parameters arising from the post-inflationary era are depicted by solid, short dotted and dot-dashed lines. Namely, the solid [dot-dashed] lines correspond to the lower [most conservative upper] bound on Y_B [$Y_{\bar{G}}$] in Eq. (4.20) [Eq. (4.21)].



INPUT PARAMETERS		OUTPUT PARAMETERS				
$M_{3\hat{\nu}^c}$ (GeV)	$-\delta$	λ (10^{-2})	$M_{2\hat{\nu}^c}$ (10^{11} GeV)	$\sin^2 \theta_{23}$ (10^{-2})	ϑ (10^{-2})	m_{2D} (GeV)
10^{15}	$\pi/3.5$	0.1 – 6.2	1.5 – 132	45.7 – 46.5	1.2 – 13	1.9 – 21.1
		6.6 – 25	9.5 – 142	44 – 46	3.6 – 1.4	5.7 – 21.9
$6 \cdot 10^{14}$	$\pi/2.5$	0.1 – 6.2	0.9 – 97	44.8 – 45.6	2 – 17	1.5 – 14
		6.6 – 25	7.7 – 94	45.3 – 47	4.7 – 12	4 – 10

Figure 3: Allowed values of $M_{2\hat{\nu}^c}$ versus λ , for the input quantities listed in the table above, $\lambda_H = \lambda_{\bar{H}} = 0.5$, $k_S = 1$ and $y_{33} = 0.5$ when the inflaton can decay into $\hat{\nu}_2^c$'s. The conventions adopted for the types and the color of the various lines are also shown.

Since we use $|\delta_{\text{eff}}| = 1$, it is clear from Eqs. (4.8) and (4.11) that values of $M_{1\hat{\nu}^c}$ above the solid line are compatible with the current data in Eq. (4.20) for conveniently adjusting $|\delta_{\text{eff}}| \leq 1$. However the values of $M_{1\hat{\nu}^c}$ can be restricted by the bounds of Eq. (4.21). Specifically we obtain $Y_{\tilde{G}} \simeq (0.1 - 1) \cdot 10^{-12}$ [$Y_{\tilde{G}} \simeq (0.5 - 1) \cdot 10^{-13}$] in the [gray] dark gray area. On the other hand, the kinematical condition depicted by a short dotted line – see Eq. (4.16) – puts the upper bound on $M_{1\hat{\nu}^c}$ in the upper right corners of the allowed region. As anticipated above, this region has two disconnected branches. In the left [right] branch, the first [second] term in Eq. (4.3) dominates. All in all we obtain

$$0.39 \lesssim M_{1\hat{\nu}^c}/10^{11} \text{ GeV} \lesssim 154 \text{ for } 0.001 \lesssim \lambda \lesssim 0.062, \quad (4.23a)$$

$$154 \gtrsim M_{1\hat{\nu}^c}/10^{11} \text{ GeV} \gtrsim 4.32 \text{ for } 0.062 \lesssim \lambda \lesssim 0.25. \quad (4.23b)$$

The overall minimal [maximal] $M_{1\hat{\nu}^c}$ can be found in the left lower [upper right] corner of the allowed region. Obviously, the maximal allowed $M_{1\hat{\nu}^c} \simeq m_1/2$ is obtained for $0.02 \lesssim \lambda \lesssim 0.062$ and $0.062 \lesssim \lambda \lesssim 0.25$. This region gives also a lower bound on $|\delta_{\text{eff}}|$, $|\delta_{\text{eff}}| \gtrsim 1.6 \cdot 10^{-4}$.

Trying to compare, finally, the resulting allowed parameter space here in the $\lambda - M_{1\hat{\nu}^c}$ plane with the one allowed within the models of HI [15] – see Fig. 2 of Ref. [65], where the coupling constant κ corresponds to λ – we remark that in our case (i) higher λ 's and $M_{1\hat{\nu}^c}$'s are allowed and (ii) there is an additional minor slice of allowed parameters exclusively due to the SUGRA induced decay channel found in Eq. (4.3).

4.3.2. Decay of the inflaton into $\hat{\nu}_2^c$. In this case, our cosmological setting depends on the following input parameters:

$$\lambda, c_{\mathcal{R}}, M_{2\hat{\nu}^c}, M_{3\hat{\nu}^c} \text{ and } \delta.$$

In our numerical program, for every λ and $c_{\mathcal{R}}$ consistent with the inflationary requirements of Sec. 3.2, we can resolve Eq. (4.14) w.r.t m_{2D} and ϑ , if we use $M_{2\hat{\nu}^c}$ and δ as input parameters – recall that m_{3D} is determined by Eq. (4.19). Diagonalizing m_{ν} and employing Eqs. (4.8) and (4.12) to estimate Y_B , we can restrict the parameters through Eqs. (4.18) and (4.20). In order to compare the value of $\sin^2 \theta_{23}$ extracted at the leptogenesis scale, T_{rh} , with the low energy experimental result of Eq. (4.18), we solve the relevant renormalization group equations following Ref. [60]. We remark that $\sin^2 \theta_{23}$ increases by almost 8% due to these renormalization effects.

In Fig. 3 we display the allowed values of $M_{2\hat{\nu}^c}$ versus λ for various $M_{3\hat{\nu}^c}$ and δ 's indicated on the left upper corner of the graph. The obtained allowed ranges of several other quantities involved are arranged in the Table below the graph. Along the displayed curves the central value of Y_B in Eq. (4.20) is achieved and we obtain $T_{\text{rh}} \simeq (0.7 - 2.9) \cdot 10^9$ GeV which is translated as $Y_{\tilde{G}} \simeq (1.3 - 5.5) \cdot 10^{-13}$ via Eq. (4.10). From our results we observe that increasing $M_{3\hat{\nu}^c}$ entails an increase of $M_{2\hat{\nu}^c}$ too whereas $-\delta$ approaches $\pi/4$ – see Eq. (4.12) – and increases as $M_{2\hat{\nu}^c}$ drops in order Eq. (4.18) to be met. The resulting m_{2D} turns out to be in the range $(1.5 - 21.9)$ GeV which is larger than the mass of the charm quark at T_{rh} , $m_c \simeq 0.427$ GeV. Therefore within our scheme the $SU(4)_C$ symmetry does not hold in the up sector of the second family.

As for the case of Sec. 4.3.1, we obtain two separate branches of allowed parameters, $h_* \geq m_{\text{P}}$ for $\lambda \leq 0.0037$, whereas Eq. (3.28a) is satisfied for $\lambda \leq 0.016$ – Eq. (3.28b) is valid for the used λ 's, see Sec. 3.3. Finally, it is remarkable that the assumptions on $M_{1\hat{\nu}^c}$, $T_{\text{rh}} < M_{1\hat{\nu}^c} \ll M_{2\hat{\nu}^c}$ can be fulfilled in a wide range, i.e., $7 \cdot 10^8 < M_{1\hat{\nu}^c}/\text{GeV} < 10^{11}$.

5 CONCLUSIONS

In this paper we attempted to embed within a realistic GUT, based on the PS gauge group, one of the recently formulated [10] SUSY models of chaotic inflation with non-minimal coupling to gravity. We showed that the model not only supports non-MHI driven by the radial component of the Higgs field, but it also leads to the spontaneous breaking of the PS gauge group to the SM one with the GUT breaking v.e.v identified with the SUSY GUT scale and without overproduction of monopoles. Moreover, within our model, we can resolve the strong CP and the μ problems of the MSSM via a Peccei-Quinn symmetry breaking transition. Inflation is followed by a reheating phase, during which the inflaton can decay into the lightest or the next-to-lightest RH neutrino allowing, thereby for non-thermal leptogenesis to occur via the subsequent decay of the RH neutrinos. Although other decay channels to the SM particles via non-renormalizable interactions are also activated, we showed that, in both cases, the production of the required by the observations BAU can be reconciled with the observational constraints on the inflationary observables and the \tilde{G} abundance, provided that the (unstable) \tilde{G} masses are greater than 10 TeV. In the first inflaton-decay scenario, we restrict the lightest RH neutrino mass to values of the order $(10^{11} - 10^{13})$ GeV whereas in the second scenario, extra restrictions from the light neutrino data and the $SU(4)_C$ factor of the adopted GUT gauge group can be also met for masses of the heaviest [next-to-lightest] RH neutrino of the order of 10^{15} GeV $[(10^{11} - 10^{13})$ GeV].

Finally, we would like to point out that, although we have restricted our discussion on the PS gauge group, non-MHI analyzed in our paper has a much wider applicability. It can be realized within other GUTs, which may (as in the case of G_{PS}) or may not lead to the formation of cosmic defects. If we adopt another GUT gauge group, the inflationary predictions and the post-inflationary evolution are expected to be quite similar to the ones discussed here with possibly different analysis of the stability of the inflationary trajectory, since different Higgs superfield representations may be involved in implementing gauge symmetry breaking to G_{SM} – see, e.g., Ref. [66] which appeared when this work was under completion.

ACKNOWLEDGEMENT

We would like to cordially thank G. Lazarides, Q. Shafi and J. Vergados for helpful discussions and Y. Watanabe for an enlightening correspondence.

APPENDIX A: DERIVATION OF THE MASS SPECTRUM DURING NON-MHI

In this Appendix, we describe the derivation of the mass spectrum of the model when the radial component, h , of the fields $\nu_H^c, \bar{\nu}_H^c$ slowly rolls down \widehat{V}_{HI} , breaking G_{PS} down to G_{SM} . We explain the results summarized in Table 2, working exclusively in the EF. We demonstrate below the origin of the masses of the scalars (Sec. A.1), gauge bosons (Sec. A.2) and fermions (Sec. A.3).

A.1 MASSES FOR THE SCALARS

Expanding \widehat{V}_{HI} in Eq. (3.12) to quadratic order in the fluctuations around the trajectory in Eq. (3.4), for given h , we obtain

$$\begin{aligned} \widehat{V}_{\text{HI}} &= \widehat{V}_{\text{HI}0} + \frac{1}{2} m_{\widehat{S}}^2 \widehat{S}^2 + \frac{1}{2} m_{\widehat{\theta}_\nu}^2 \widehat{\theta}_\nu^2 + \frac{1}{2} \begin{pmatrix} \widehat{\theta} & \widehat{\theta} \end{pmatrix} M_\theta^2 \begin{pmatrix} \widehat{\theta} \\ \widehat{\theta} \end{pmatrix} \\ &+ \frac{1}{2} \sum_x \left(\begin{pmatrix} \widehat{x}_1 & \widehat{x}_1 \end{pmatrix} M_{x1}^2 \begin{pmatrix} \widehat{x}_1 \\ \widehat{x}_1 \end{pmatrix} + \begin{pmatrix} \widehat{x}_2 & \widehat{x}_2 \end{pmatrix} M_{x2}^2 \begin{pmatrix} \widehat{x}_2 \\ \widehat{x}_2 \end{pmatrix} \right), \end{aligned} \quad (\text{A.1})$$

where $x = u, e, d$ and g and the decomposition of the scalar fields into real and imaginary parts is shown in Eq. (3.7). The various mass-squared matrices involved in Eq. (A.1) are found to be

$$M_\theta^2 = \begin{pmatrix} 1 & 1 \\ 1 & 1 \end{pmatrix} m_{\widehat{\theta}_+}^2 / 2, \quad M_{g1}^2 = M_{g2}^2 = \begin{pmatrix} m_g^2 & 0 \\ 0 & m_g^2 \end{pmatrix}, \quad M_{y1}^2 = \begin{pmatrix} m_{\widehat{y}1}^2 & m_{\widehat{y}2}^2 \\ m_{\widehat{y}2}^2 & m_{\widehat{y}1}^2 \end{pmatrix}, \quad (\text{A.2a})$$

$$M_{y2}^2 = \begin{pmatrix} m_{\widehat{y}1}^2 & -m_{\widehat{y}2}^2 \\ -m_{\widehat{y}2}^2 & m_{\widehat{y}1}^2 \end{pmatrix}, \quad M_{d1}^2 = \begin{pmatrix} m_{\widehat{d}1}^2 & m_{\widehat{d}2}^2 \\ m_{\widehat{d}2}^2 & m_{\widehat{d}3}^2 \end{pmatrix} \quad \text{and} \quad M_{d2}^2 = \begin{pmatrix} m_{\widehat{d}1}^2 & -m_{\widehat{d}2}^2 \\ -m_{\widehat{d}2}^2 & m_{\widehat{d}3}^2 \end{pmatrix} \quad (\text{A.2b})$$

where $y = u$ and e and $m_{\widehat{\theta}_+}^2, m_g^2, m_{\widehat{y}1}^2$ and also $m_{\widehat{S}}^2$ are presented in Table 2. The elements of the remaining matrices above are found to be

$$m_{\widehat{y}1}^2 = m_{\text{P}}^2 x_h^2 (3g^2 f + \lambda^2 x_h^2) / 24f^2, \quad m_{\widehat{y}2}^2 = -m_{\text{P}}^2 x_h^2 (\lambda^2 (x_h^2 - 6) + 3g^2 f) / 24f^2, \quad (\text{A.3a})$$

$$m_{\widehat{d}1}^2 = m_{\text{P}}^2 x_h^2 (\lambda^2 x_h^2 + 24\lambda_H^2 f) / 24f^2, \quad m_{\widehat{d}2}^2 = -\lambda^2 m_{\text{P}}^2 x_h^2 (x_h^2 - 6) / 24f^2, \quad (\text{A.3b})$$

whereas $m_{\widehat{d}3}^2$ is the same as $m_{\widehat{d}1}^2$ but with λ_H replaced by $\lambda_{\bar{H}}$. To simplify our formulae below, we take $\lambda_H \simeq \lambda_{\bar{H}}$. The various masses squared in Eqs. (A.2a) and (A.2b) originate mainly from \widehat{V}_{HF} in Eq. (3.2). Additional contributions from V_{HD}/f^2 in Eq. (2.15) arise for $m_{\widehat{\theta}_+}^2$ and $m_{\widehat{y}2}^2$. The orthogonal matrix U_K , which diagonalizes M_K in Eq. (3.9), diagonalizes M_θ^2 too. We find the following eigenstates

$$\widehat{\theta}_\pm = \frac{1}{\sqrt{2}} \begin{pmatrix} \widehat{\theta} \\ \pm \widehat{\theta} \end{pmatrix} \quad (\text{A.4})$$

with eigenvalues $m_{\widehat{\theta}_+}^2$ and $m_{\widehat{\theta}_-}^2 = 0$ respectively. The second eigenstate corresponds to the Goldstone mode absorbed by A^\perp – see Sec. A.2 – via the Higgs mechanism. Upon diagonalization of M_{x1}^2 and M_{x2}^2 with $x = u, e$ and d , we obtain the eigenvalues

$$m_{\widehat{x}\pm}^2 = m_{\widehat{x}1}^2 \pm m_{\widehat{x}2}^2 \quad (\text{A.5})$$

which correspond to the following eigenstates respectively:

$$\hat{x}_{1\pm} = \frac{1}{\sqrt{2}} (\hat{x}_1 \pm \hat{x}_1) \quad \text{and} \quad \hat{x}_{2\mp} = \frac{1}{\sqrt{2}} (\hat{x}_2 \mp \hat{x}_2) \quad \text{with} \quad x = u^a, e \text{ and } d. \quad (\text{A.6})$$

Note that $m_{\hat{x}_+}^2 = m_{\hat{x}_0}^2 = \lambda^2 m_P^2 x_h^2 / 4f^2 \ll m_{\hat{x}_-}^2$ for $x = u$ (3 colors) and $x = e$ are the masses squared of the Goldstone bosons \hat{x}_{1+} and \hat{x}_{2-} which are absorbed by A_C^\pm (3 colors) and A_R^\pm – see Sec. A.2 – via the Higgs mechanism. The remaining $m_{\hat{x}_\pm}^2$'s are listed in Table 2.

A.2 MASSES FOR THE GAUGE BOSONS

Some of the gauge bosons A_C^a and A_R^m acquire masses from the lagrangian terms – cf. Ref. [39]:

$$K_{\alpha\bar{\beta}} \left((D_\mu \bar{H}^{c*})^\alpha (D^\mu \bar{H}^{c\Gamma})^{\bar{\beta}} + (D_\mu H^{c\dagger})^\alpha (D^\mu H^c)^{\bar{\beta}} \right) = \frac{1}{2} m_\pm^2 \left(\left(\sqrt{\frac{3}{2}} A_{C\mu}^{15} - A_{R\mu}^3 \right) \left(\sqrt{\frac{3}{2}} A_C^{15\mu} - A_R^{3\mu} \right) + 2A_{R\mu}^+ A_R^{\mu-} + 2 \sum_{a=1}^3 A_{C\mu}^{a+} A_C^{\mu a-} \right), \quad (\text{A.7})$$

where m_\pm are given in Table 2. The action of D_μ on H^c and \bar{H}^c is as follows

$$D_\mu \bar{H}^{c\Gamma} = \partial_\mu \bar{H}^{c\Gamma} + ig \left(\sum_{a=1}^{15} T_C^a A_C^a \bar{H}^{c\Gamma} + \sum_{m=1}^3 T_R^m A_R^m \bar{H}^{c\Gamma} \right) \quad (\text{A.8a})$$

$$D_\mu H^c = \partial_\mu H^c - ig \left(\sum_{a=1}^{15} T_C^{a*} A_C^a H^c + \sum_{m=1}^3 T_R^{m*} A_R^m H^c \right), \quad (\text{A.8b})$$

and we have defined the following normalized gauge fields:

$$A_C^{a\pm} = \frac{1}{\sqrt{2}} (A_C^{7+2a} \pm i A_C^{8+2a}) \quad \text{for } a = 1, 2, 3 \quad \text{and} \quad A_R^\pm = \frac{1}{\sqrt{2}} (A_R^1 \pm i A_R^2). \quad (\text{A.9})$$

The first term of the RHS of Eq. (A.7) can be written as

$$\frac{1}{2} m_\pm^2 \begin{pmatrix} A_C^{15\mu} & A_R^{3\mu} \end{pmatrix} M_{\text{CR}} \begin{pmatrix} A_C^{15\mu} \\ A_R^{3\mu} \end{pmatrix} = \frac{1}{2} m_\pm^2 A^{\perp\mu} A_\mu^\perp, \quad (\text{A.10})$$

where $m_\pm^2 = 5m_\pm^2/2$ – see Table 2 – since

$$M_{\text{CR}} = \begin{pmatrix} 3/2 & -\sqrt{3/2} \\ -\sqrt{3/2} & 1 \end{pmatrix} \quad \text{and} \quad U_{\text{CR}} M_{\text{CR}} U_{\text{CR}}^\text{T} = \text{diag}(5/2, 0) \quad (\text{A.11})$$

with

$$U_{\text{CR}} = \begin{pmatrix} -\sqrt{3/5} & \sqrt{2/5} \\ \sqrt{2/5} & \sqrt{3/5} \end{pmatrix} \quad \text{and} \quad \begin{pmatrix} A^\perp \\ A^\parallel \end{pmatrix} = U_{\text{CR}} \begin{pmatrix} A_C^{15} \\ A_R^3 \end{pmatrix}. \quad (\text{A.12})$$

Therefore, from Eqs. (A.7) and (A.10), we can infer that 9 gauge bosons (A^\perp , $A_C^{a\pm}$ and A_R^\pm) become massive, absorbing the massless modes $\hat{\theta}_-$, \hat{u}_{1+}^a , \hat{u}_{2-}^a , \hat{e}_{1+} and \hat{e}_{2-} , whereas A^\parallel , which remains massless, can be interpreted as the B boson associated with the $U(1)_Y$ factor of G_{SM} .

A.3 MASSES FOR THE FERMIONS

The lagrangian kinetic terms of the chiral fermions ψ_x with $x = \nu, e, u, d, g, \bar{\nu}, \bar{e}, \bar{u}, \bar{d}, \bar{g}$, which are associated with the superfields $\nu_H^c, e_H^c, u_H^c, d_H^c, g^c, \bar{\nu}_H^c, \bar{e}_H^c, \bar{u}_H^c, \bar{d}_H^c, \bar{g}^c$ respectively, are

$$\begin{aligned} K_{\alpha\bar{\beta}} \bar{\psi}^\alpha \bar{\sigma}^\mu D_\mu \psi^{\bar{\beta}} &= \frac{1}{f^2} \begin{pmatrix} \bar{\psi}_\nu & \bar{\psi}_{\bar{\nu}} \end{pmatrix} M_K \begin{pmatrix} \psi_\nu \\ \psi_{\bar{\nu}} \end{pmatrix} + \sum_y \frac{1}{f} \bar{\psi}_y \bar{\sigma}^\mu D_\mu \psi_y \\ &= \bar{\psi}_{\nu+} \bar{\sigma}^\mu D_\mu \hat{\psi}_{\nu+} + \bar{\psi}_{\nu-} \bar{\sigma}^\mu D_\mu \hat{\psi}_{\nu-} + \sum_y \bar{\psi}_y \bar{\sigma}^\mu D_\mu \hat{\psi}_y, \end{aligned} \quad (\text{A.13})$$

where we have used Eq. (3.9), and the normalized spinors are defined as follows

$$\widehat{\psi}_{\nu+} = \frac{\sqrt{f}}{f} \psi_{\nu+}, \quad \widehat{\psi}_{\nu-} = \frac{\psi_{\nu-}}{\sqrt{f}} \quad \text{with} \quad \psi_{\nu\pm} = \frac{1}{\sqrt{2}} (\psi_{\bar{\nu}} \pm \psi_{\nu}) \quad \text{and} \quad \widehat{\psi}_y = \frac{\psi_y}{\sqrt{f}} \quad (\text{A.14})$$

with $y = e, u, d, g, \bar{e}, \bar{u}, \bar{d}$, and \bar{g} . In Eq. (A.13) the contraction between two Weyl spinors is suppressed; the Pauli matrices $\bar{\sigma}^\mu$ and the action of D_μ on ψ^α are specified in Ref. [3, 42].

Having defined the normalized spinors, we can proceed with the derivation of the fermionic mass spectrum of our model. The masses of the chiral fermions can be found applying the formula [3, 42]:

$$m_{\alpha\beta} = e^{K/2m_{\text{P}}^2} \left(W_{\text{HPS}\alpha\beta} + \frac{1}{m_{\text{P}}^2} (K_{\alpha\beta} W_{\text{HPS}} + K_\alpha F_\beta + K_\beta F_\alpha) - \Gamma_{\alpha\beta}^\gamma F_\gamma \right) \quad (\text{A.15})$$

with $\Gamma_{\alpha\beta}^\gamma = K^{\gamma\bar{\gamma}} \partial_\alpha K_{\beta\bar{\gamma}}$, $W_{\text{HPS}\alpha\beta} = W_{\text{HPS},\phi^\alpha\phi^\beta}$, $K_\alpha = K_{,\phi^\alpha}$ and F_α as defined below Eq. (3.2). Upon diagonalization of the relevant mass matrix, we obtain the eigenvalues $m_{\widehat{\psi}_{S\nu}}$, $m_{\widehat{\psi}_{gd}}$ and $m_{\widehat{\psi}_{g\bar{d}}}$, listed in Table 2, corresponding to the following eigenstates

$$\widehat{\psi}_{S\nu\pm} = \frac{1}{\sqrt{2}} (\widehat{\psi}_S \pm \widehat{\psi}_{\nu+}), \quad \widehat{\psi}_{g\bar{d}\pm}^a = \frac{1}{\sqrt{2}} (\widehat{\psi}_{\bar{g}}^a \pm \widehat{\psi}_{\bar{d}}^a) \quad \text{and} \quad \widehat{\psi}_{gd\pm}^a = \frac{1}{\sqrt{2}} (\widehat{\psi}_g^a \pm \widehat{\psi}_d^a). \quad (\text{A.16})$$

We remark that W_{HPS} in Eq. (2.9) does not give rise to mass terms for fermions in the sectors $u_H^c - \bar{u}_H^c$ and $e_H^c - \bar{e}_H^c$. However fermion masses also arise from the lagrangian terms

$$\begin{aligned} & -i\sqrt{2}gK_{\alpha\bar{\beta}} \left(\sum_{a=1}^{15} \bar{\lambda}_C^a (\bar{\psi}_{H^c}^\alpha (T^a \bar{H}^{c\Gamma})^{\bar{\beta}} - \bar{\psi}_{H^c}^{\alpha\Gamma} (T^{a*} H^c)^{\bar{\beta}}) + \right. \\ & \left. \sum_{m=1}^3 \bar{\lambda}_R^m (\bar{\psi}_{H^c}^\alpha (T^m \bar{H}^{c\Gamma})^{\bar{\beta}} - \bar{\psi}_{H^c}^{\alpha\Gamma} (T^{m*} H^c)^{\bar{\beta}}) + \text{h.c.} \right), \end{aligned} \quad (\text{A.17})$$

where λ_C^a [λ_R^m], is the gaugino corresponding to the generator T_C^a [T_R^m] and ψ_{H^c} , ψ_{H^c} represent the chiral fermions belonging to the superfields \bar{H}^c , H^c respectively. Concentrating on T_C^{15} , T_R^3 , we obtain

$$\begin{aligned} & -i\sqrt{2}g \left(\bar{\lambda}_C^{15} \begin{pmatrix} \bar{\psi}_\nu & \bar{\psi}_{\bar{\nu}} \end{pmatrix} \frac{M_K}{f^2} \begin{pmatrix} -T_C^{15*} H^c \\ T_C^{15} H^{c\Gamma} \end{pmatrix} + \bar{\lambda}_C^{15} \begin{pmatrix} \bar{\psi}_\nu & \bar{\psi}_{\bar{\nu}} \end{pmatrix} \frac{M_K}{f^2} \begin{pmatrix} -T_R^{3*} H^c \\ T_R^3 H^{c\Gamma} \end{pmatrix} \right) + \text{h.c.} = \\ & \frac{igh}{2f} \frac{\psi_{\bar{\nu}} - \psi_\nu}{\sqrt{2}} \left(-\sqrt{\frac{3}{2}} \lambda_C^{15} + \lambda_R^3 \right) + \text{h.c.} = -im_\perp \widehat{\psi}_{\nu-} \lambda^\perp + \text{h.c.} \quad \text{with} \quad \begin{pmatrix} \lambda^\perp \\ \lambda^\parallel \end{pmatrix} = U_{\text{CR}} \begin{pmatrix} \lambda_C^{15} \\ \lambda_R^3 \end{pmatrix}. \end{aligned}$$

Therefore, we obtain a Dirac mass term between the chiral fermion $\widehat{\psi}_{\nu-}$ and the gaugino $-i\lambda^\perp$, whereas a Dirac spinor composed by the combination of $\widehat{\psi}_{\nu+}$ and $-i\lambda^\parallel$ remains massless and can be interpreted as the Goldstino which signals the (spontaneous) SUSY breaking along the direction of Eq. (3.4).

Similarly, focusing on the directions T_C^{8+2a} with $a = 1, 2, 3$ and T_R^1 and T_R^2 , we obtain the mass terms

$$i \frac{gh}{2\sqrt{f}} \left(\sum_{a=1}^3 (\widehat{\psi}_u^a \lambda_C^{a+} - \widehat{\psi}_{\bar{u}}^a \lambda_C^{a-} + \text{h.c.}) + (\widehat{\psi}_e \lambda_R^- - \widehat{\psi}_{\bar{e}} \lambda_R^+ + \text{h.c.}) \right), \quad (\text{A.18})$$

where we have defined the following combinations of gauginos

$$\lambda_C^{a\pm} = \frac{1}{\sqrt{2}} (\lambda_C^{7+2a} \pm i\lambda_C^{8+2a}) \quad \text{for} \quad a = 1, 2, 3 \quad \text{and} \quad \lambda_R^\pm = \frac{1}{\sqrt{2}} (\lambda_R^1 \pm i\lambda_R^2) \quad (\text{A.19})$$

in agreement with the definition of the corresponding gauge bosons in Eq. (A.9). Therefore, the chiral fermions $\widehat{\psi}_u^a$ and $\widehat{\psi}_{\bar{u}}^a$ [$\widehat{\psi}_e$ and $\widehat{\psi}_{\bar{e}}$] combine with $\lambda_C^{a\pm}$ [λ_R^\pm] to form two Dirac (or four Weyl) fermions with mass m_\pm as one deduces from Eq. (A.18). This completes the derivation of the spectrum of the model along the inflationary trajectory of Eq. (3.4).

APPENDIX B: INFLATON OSCILLATIONS AFTER NON-MHI

In this Appendix we discuss various (p)reheating mechanisms [51] which could become competitive with the perturbative decay of the inflaton to lighter degrees of freedom, as analyzed in Sec. 4. Indeed, in certain regions of the parameter space, the process of reheating in this theory can be quite complex. After the end of non-MHI, the inflaton develops a tachyonic mass, crosses an inflection point and enters into a phase of damped oscillations. As pointed out in Ref. [52], where a similar potential is investigated, the particle production due to tachyonic preheating is not significant because the passage of the inflaton through this region is very short. During the subsequent oscillations, perturbative production of superheavy bosons – i.e., bosons with masses at the SUSY vacuum proportional to M_{PS} – is not possible, since these particles are heavier than the inflaton at the global minima of its potential as shown in Table 3. Therefore effects of narrow parametric resonance [51] are also absent. However, if the initial amplitude of the inflaton oscillations is large enough, it may pass through zero, $h = 0$, where these bosons are effectively light and can be produced through (non-perturbative) instant preheating [53], as we discuss in Sec. B.2 below. We first study the dynamics of the inflaton's oscillations in Sec. B.1.

B.1 DYNAMICS OF THE INFLATON OSCILLATIONS

The cosmological evolution of $\hat{h}(h)$ in the EF is governed by the equation of motion:

$$\ddot{\hat{h}} + 3\hat{H}\dot{\hat{h}} + \hat{V}_{\text{HI0},\hat{h}} = 0 \quad (\text{B.1})$$

where \hat{H} is the Hubble parameter in the EF and \hat{V}_{HI0} is given in Eq. (3.5) – recall that the dot denotes derivation w.r.t. the cosmic time t and $h = \text{Re}(\nu_H^c + \bar{\nu}_H^c)/2$ along the direction of Eq. (3.4). In the LHS of Eq. (B.1), we neglect the damping term $\Gamma_1 \dot{\hat{h}}$ which is important only at the stage of rapid oscillations of \hat{h} near one of the minima of \hat{V}_{HI0} [51]. Note that contrary to the case of the potential analyzed in Ref. [52], the minima of \hat{V}_{HI0} lie at $|h| = 2M_{\text{PS}} \gg 0$ and \hat{V}_{HI0} has a maximum at $h = 0$ with

$$\hat{V}_{\text{HI0}}(h = 0) = \hat{V}_0 = \lambda^2 M_{\text{PS}}^4 \quad (\text{B.2})$$

which can not be ignored. Due to these features, the quadratic approximation to \hat{V}_{HI0} is not accurate enough for the description of the h post-inflationary evolution.

The solution of Eq. (B.1) can be facilitated if we use as independent variable the number of e-foldings \hat{N} defined by

$$\hat{N} = \ln\left(\hat{R}/\hat{R}_i\right) \Rightarrow \dot{\hat{N}} = \hat{H} \text{ and } \dot{\hat{H}} = \hat{H}'\hat{H}. \quad (\text{B.3})$$

Here the prime denotes derivation w.r.t. \hat{N} , $\hat{R}(t)$ is the EF scale factor and \hat{R}_i is its value at the commencement of non-MHI, which turns out to be numerically irrelevant. Converting the time derivatives to derivatives w.r.t. \hat{N} , Eq. (B.1) is equivalent to the following system of two first order equations

$$F_h = J\hat{H}\hat{R}^3 h' \text{ and } J\hat{H}F_h' = -\hat{V}_{\text{HI0},h}\hat{R}^3 \text{ with } F_h = \dot{\hat{h}}\hat{R}^3. \quad (\text{B.4})$$

This system can be solved numerically by taking

$$\hat{H} = \frac{1}{\sqrt{3}m_{\text{P}}} \left(F_h^2/2R^6 + \hat{V}_{\text{HI0}} \right)^{1/2} \quad (\text{B.5})$$

and imposing the initial conditions (at $\hat{N} = 0$) $h(0) = (0.5 - 2.5)m_{\text{P}}$ and $h'(0) = 0$. We checked that our results are pretty stable against variation of $h(0)$.

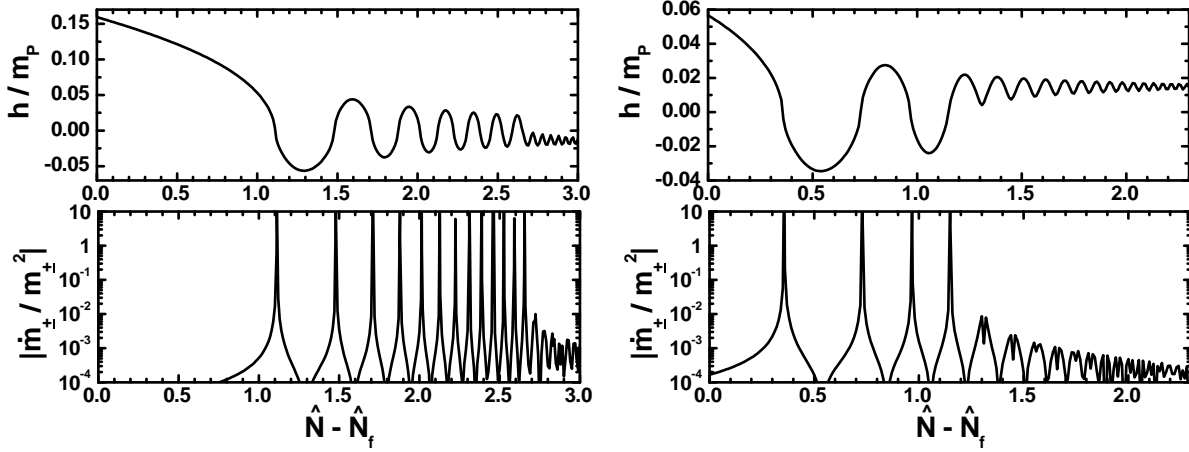


Figure 4: The evolution of the quantities h/m_P (upper plots) and $|\dot{m}_\pm/m_\pm^2|$ (lower plots) as functions of $\hat{N} - \hat{N}_f$ for $\lambda = 0.0037$ and $c_{\mathcal{R}} = 81$ (left panel) or $\lambda = 0.01$ and $c_{\mathcal{R}} = 235$ (right panel).

During non-MHI we have $\hat{H} \simeq \hat{H}_{\text{HIO}}$ and the results of Eqs. (3.20) and (3.23) are well verified. Soon after the end of non-MHI, we obtain $\hat{H} \simeq \hat{H}_{\text{HIO}} e^{-3(\hat{N} - \hat{N}_f)/2}$ – with \hat{N}_f being the value of \hat{N} at the end of non-MHI – and h enters into an oscillatory phase with initial amplitude equal to h_f given by Eq. (3.19). Since the value of \hat{V}_{HIO} at the end of inflation, V_{HIO} is larger than the value of \hat{V}_{HIO} at its local maximum $h = 0$, \hat{V}_0 , we expect that h crosses zero at least once during its evolution. However, as can be deduced from Eqs. (3.19) and (3.23), lowering λ increases h_f but decreases \hat{V}_0 . Therefore the passage of h through zero is facilitated.

The intuitive results above can be established and refined through the numerical solution of Eq. (B.4), during the h oscillations, depicted in the upper plots of Fig. 4. Namely in left [right] plot we present the evolution of h as a function of $\hat{N} - \hat{N}_f$ for $\lambda = 0.0037$ and $c_{\mathcal{R}} = 81$ [$\lambda = 0.01$ and $c_{\mathcal{R}} = 235$]. In both cases, we see that h , decreasing slowly from its value $h_f = 0.152$ [$h_f = 0.056$] for $\lambda = 0.0037$ [$\lambda = 0.01$], passes from the minimum of \hat{V}_{HIO} at $h = 2M_{\text{PS}}$ and then climbs up the hill of \hat{V}_{HIO} at $h = 0$, falls towards the other minimum of \hat{V}_{HIO} at $h = -2M_{\text{PS}}$ until it reaches a maximal value and oscillates backwards. This path is followed some times until h falls finally into one of the minima of \hat{V}_{HIO} at $h = -2M_{\text{PS}}$ [$h = 2M_{\text{PS}}$] for $\lambda = 0.0037$ [$\lambda = 0.01$] – performing damped oscillations about it. In other words, h oscillates initially around the local maximum of \hat{V}_{HIO} and then about one of the two SUSY vacua. The number of passages through zero increases as λ decreases – it is equal to 4 [12] for $\lambda = 0.01$ [$\lambda = 0.0037$]. Solving repetitively Eq. (B.4) we notice that h ceases to cross $h = 0$ for $\lambda > 0.088$.

B.2 INSTANT PREHEATING

Whenever h crosses zero particle production may occur via instant preheating [53]. This mechanism is activated when the h -dependent effective masses, m_{eff} , of the produced particles violate the adiabaticity criterion, according to which

$$|\dot{m}_{\text{eff}}/m_{\text{eff}}^2| = \left| \frac{\hat{H} m'_{\text{eff}}}{m_{\text{eff}}^2} \right| \ll 1. \quad (\text{B.6})$$

Here, m_{eff} represents collectively the masses of superheavy bosons with masses proportional to gM_{PS} , $\lambda_H M_{\text{PS}}$ or $\lambda_{\bar{H}} M_{\text{PS}}$ – see Table 2. We focus on the production of these bosons since these can subsequently decay efficiently to the light SM particles altering drastically the picture of the usual perturbative reheating. On the contrary, the scalars of the $S - \nu_H^c - \bar{\nu}_H^c$ sector with masses proportional to λM_{PS} have suppressed decay modes to the RH neutrinos only. Taking as an example $m_{\text{eff}} = m_\pm$ we

plot in the lower plots of Fig. 4 the evolution of $|\hat{m}_{\pm}/m_{\pm}^2|$ as a function of $\hat{N} - \hat{N}_f$ for $\lambda = 0.0037$ and $c_{\mathcal{R}} = 81$ [$\lambda = 0.01$ and $c_{\mathcal{R}} = 235$] – see left [right] plot. We observe that Eq. (B.6) is violated more frequently as λ drops since the passages of h through zero become also more frequent. From the results of our numerical treatment we find that Eq. (B.6) holds during the whole post-inflationary evolution of h for $\lambda > 0.045$ whereas it fails more than 40 times for $\lambda < 0.001$.

The produced this way superheavy bosons acquire a large mass while the inflaton increases towards its maximum amplitude and start to decay into all lighter particles within almost half oscillation of the inflaton, rapidly depleting their occupation numbers. As shown in Ref. [52] an efficient transfer of energy from h to the superheavy bosons requires a rather large (let say 50 – 70) number of passages of h through zero. Meanwhile effect of backreaction of the produced particles on the h condensate may become significant and a more involved numerical study of the process is imperative. Trying to deliberate our leptogenesis scenario from such a complicate situation, we impose the indicative lower bound $\lambda \geq 0.001$ – which can be translated as a bound $c_{\mathcal{R}} \geq 21$ via Eq. (3.23) – above which our estimations in Sec. 4 are more or less independent of the preheating effects. We hope to return to the analysis of $\lambda < 0.001$ region in the future.

REFERENCES

- [1] J.L. Cervantes-Cota and H. Dehnen, *Nucl. Phys.* **B442**, 391 (1995) [astro-ph/9505069];
F.L. Bezrukov and M. Shaposhnikov, *Phys. Lett. B* **659**, 703 (2008) [arXiv:0710.3755];
A.O. Barvinsky *et al.*, *J. Cosmol. Astropart. Phys.* **11**, 021 (2008) [arXiv:0809.2104];
A. De Simone, M.P. Hertzberg and F. Wilczek, *Phys. Lett. B* **678**, 1 (2009) [arXiv:0812.4946];
N. Okada, M. Ur Rehman and Q. Shafi, arXiv:0911.5073.
- [2] R.N. Lerner and J. McDonald, *Phys. Rev. D* **82**, 103525 (2010) [arXiv:1005.2978];
G.F. Giudice and H.M. Lee, *Phys. Lett. B* **694**, 294 (2011) [arXiv:1010.1417];
F. Bauer and D.A. Demir, *Phys. Lett. B* **698**, 425 (2011) [arXiv:1012.2900].
- [3] M.B. Einhorn and D.R.T. Jones, *J. High Energy Phys.* **03**, 026 (2010) [arXiv:0912.2718];
S. Ferrara *et al.*, *Phys. Rev. D* **82**, 045003 (2010) [arXiv:1004.0712];
H.M. Lee, *J. Cosmol. Astropart. Phys.* **08**, 003 (2010) [arXiv:1005.2735];
S. Ferrara *et al.*, *Phys. Rev. D* **83**, 025008 (2011) [arXiv:1008.2942].
- [4] I. Ben-Dayan and M.B. Einhorn, *J. Cosmol. Astropart. Phys.* **12**, 002 (2010) [arXiv:1009.2276];
K. Nakayama and F. Takahashi, *J. Cosmol. Astropart. Phys.* **11**, 009 (2010) [arXiv:1008.2956];
K. Nakayama and F. Takahashi, *J. Cosmol. Astropart. Phys.* **11**, 039 (2010) [arXiv:1009.3399].
- [5] R. Fakir and W.G. Unruh, *Phys. Rev. D* **41**, 1783 (1990);
E. Komatsu and T. Futamase, *Phys. Rev. D* **59**, 064029 (1999) [astro-ph/9901127];
S. Tsujikawa and B. Gumjudpai, *Phys. Rev. D* **69**, 123523 (2004) [astro-ph/0402185].
- [6] K. Nozari and S.D. Sadatian, *Mod. Phys. Lett. A* **23**, 2933 (2008) [arXiv:0710.0058];
K. Nozari and S. Shafizadeh, *Phys. Scripta* **82**, 015901 (2010) [arXiv:1006.1027].
- [7] T.E. Clark, B. Liu, S.T. Love and T. ter Veldhuis, *Phys. Rev. D* **80**, 075019 (2009) [arXiv:0906.5595];
R.N. Lerner and J. McDonald, *Phys. Rev. D* **80**, 123507 (2009) [arXiv:0909.0520].
- [8] S.C. Park and S. Yamaguchi, *J. Cosmol. Astropart. Phys.* **08**, 009 (2008) [arXiv:0801.1722];
C. Pallis, *Phys. Lett. B* **692**, 287 (2010) [arXiv:1002.4765];
S. Koh and M. Minamitsuji, *Phys. Rev. D* **83**, 046009 (2011) [arXiv:1011.4655].
- [9] N. Okada, M.U. Rehman and Q. Shafi, *Phys. Rev. D* **82**, 043502 (2010) [arXiv:1005.5161];
N. Okada, M.U. Rehman and Q. Shafi, *Phys. Lett. B* **520**, 701 (2011) [arXiv:1102.4747].
- [10] R. Kallosh and A. Linde, *J. Cosmol. Astropart. Phys.* **11**, 011 (2010) [arXiv:1008.3375];
A. Linde, M. Noorbala and A. Westphal, *J. Cosmol. Astropart. Phys.* **03**, 013 (2011) [arXiv:1101.2652].
- [11] C. Pallis and N. Toumbas, *J. Cosmol. Astropart. Phys.* **02**, 019 (2011) [arXiv:1101.0325].

- [12] Y.G. Kim, H.M. Lee and W.-I. Park, *J. High Energy Phys.* **08**, 126 (2011) [arXiv:1107.1113].
- [13] J.L. Cervantes-Cota and H. Dehnen, *Phys. Rev. D* **51**, 395 (1995) [astro-ph/9412032].
- [14] E. Komatsu *et al.* [WMAP Collaboration], *Astrophys. J. Suppl.* **192**, 18 (2011) [arXiv:1001.4538]
<http://lambda.gsfc.nasa.gov/product/map/dr2/parameters.cfm>.
- [15] G.R. Dvali, Q. Shafi and R.K. Schaefer, *Phys. Rev. Lett.* **73**, 1886 (1994) [hep-ph/9406319].
- [16] G. Lazarides and C. Panagiotakopoulos, *Phys. Rev. D* **52**, 559 (1995) [hep-ph/9506325];
R. Jeannerot, S. Khalil and G. Lazarides, *Phys. Lett. B* **506**, 344 (2001) [hep-ph/0103229].
- [17] G. Lazarides and A. Vamvasakis, *Phys. Rev. D* **76**, 083507 (2007) [arXiv:0705.3786].
- [18] R. Jeannerot, S. Khalil and G. Lazarides, *J. High Energy Phys.* **07**, 069 (2002) [hep-ph/0207].
- [19] R. Jeannerot, S. Khalil, G. Lazarides and Q. Shafi, *J. High Energy Phys.* **10**, 012 (2000) [hep-ph/0002151];
M. Civeletti, M.Ur Rehman, Q. Shafi and J.R. Wickman, *Phys. Rev. D* **84**, 103505 (2011) [arXiv:1104.4143].
- [20] B. Garbrecht, C. Pallis and A. Pilaftsis, *J. High Energy Phys.* **12**, 038 (2006) [hep-ph/0605264];
M. Bastero-Gil, S.F. King and Q. Shafi, *Phys. Lett. B* **651**, 345 (2007) [hep-ph/0604198];
M. Ur Rehman, V.N. Şenoğuz and Q. Shafi, *Phys. Rev. D* **75**, 043522 (2007) [hep-ph/0612023];
G. Lazarides and C. Pallis, *Phys. Rev. D* **82**, 063535 (2010) [arXiv:1007.1558].
- [21] R.A. Battye, B. Garbrecht and A. Moss, *J. Cosmol. Astropart. Phys.* **09**, 007 (2006) [astro-ph/0607339];
G. Lazarides, I.N.R. Peddie and A. Vamvasakis, *Phys. Rev. D* **78**, 043518 (2008) [arXiv:0804.3661].
- [22] G. Lazarides and C. Pallis, *Phys. Lett. B* **651**, 216 (2007) [hep-ph/0702260];
G. Lazarides and A. Vamvasakis, *Phys. Rev. D* **76**, 123514 (2007) [arXiv:0709.3362].
- [23] C. Pallis, “*High Energy Physics Research Advances*”, edited by T.P. Harrison and R.N. Gonzales (Nova Science Publishers Inc., New York, 2008) [arXiv:0710.3074].
- [24] M.Ur Rehman, Q. Shafi and J.R. Wickman, *Phys. Lett. B* **683**, 191 (2010) [arXiv:0912.4737];
M.Ur Rehman, Q. Shafi, and J.R. Wickman, *Phys. Lett. B* **688**, 75 (2010) [arXiv:0908.3896];
Q. Shafi and J.R. Wickman, *Phys. Lett. B* **696**, 438 (2011) [arXiv:1009.5340];
M. Ur Rehman, Q. Shafi and J.R. Wickman, *Phys. Rev. D* **83**, 067304 (2011) [arXiv:1012.0309].
- [25] G. Shiu and S.-H.H. Tye, *Phys. Rev. D* **58**, 106007 (1998) [hep-th/9805157];
L.L. Everett, G.L. Kane, S.F. King, S. Rigolin and L.-T. Wang, *Phys. Lett. B* **531**, 263 (2002) [hep-ph/0202100].
- [26] I. Antoniadis and G.K. Leontaris, *Phys. Lett. B* **216**, 333 (1989);
I. Antoniadis, G.K. Leontaris and J. Rizos, *Phys. Lett. B* **245**, 161 (1990).
- [27] G. Lazarides and Q. Shafi, *Phys. Rev. D* **58**, 071702 (1998) [hep-ph/9803397].
- [28] R. Peccei and H. Quinn, *Phys. Rev. Lett.* **38**, 1440 (1977);
S. Weinberg, *ibid.* **40**, 223 (1978);
F. Wilczek, *ibid.* **40**, 279 (1978).
- [29] T. Yanagida, Proceedings of the Workshop on the Unified Theory and the Baryon Number in the Universe (O. Sawada and A. Sugamoto, eds.), KEK, Tsukuba, Japan, 1979, p. 95; M. Gell-Mann, P. Ramond, and R. Slansky, Supergravity (P. van Nieuwenhuizen *et al.* eds.), North Holland, Amsterdam, 1979, p. 315; S.L. Glashow, Proceedings of the 1979 Cargese Summer Institute on Quarks and Leptons (M. Levy *et al.* eds.), Plenum Press, New York, 1980, p. 687; P. Minkowski, *Phys. Lett. B* **67**, 421 (1977); R. N. Mohapatra and G. Senjanović, *Phys. Rev. Lett.* **44**, 912 (1980).
- [30] G. Lazarides and Q. Shafi, *Phys. Lett. B* **258**, 305 (1991);
K. Kumekawa, T. Moroi and T. Yanagida, *Prog. Theor. Phys.* **92**, 437 (1994) [hep-ph/9405337];
G. Lazarides, R.K. Schaefer and Q. Shafi, *Phys. Rev. D* **56**, 1324 (1997) [hep-ph/9608256];
G. Lazarides, hep-ph/9905450.
- [31] K. Hamaguchi, *Phd Thesis* [hep-ph/0212305];
W. Buchmuller, R.D. Peccei and T. Yanagida, *Ann. Rev. Nucl. Part. Sci.* **55**, 311 (2005) [hep-ph/0502169].
- [32] G. Lazarides, Q. Shafi and N.D. Vlachos *Phys. Lett. B* **427**, 53 (1998) [hep-ph/9706385];
V.N. Şenoğuz and Q. Shafi, *Phys. Lett. B* **582**, 6 (2004) [hep-ph/0309134].

- [33] M.Yu. Khlopov and A.D. Linde, *Phys. Lett. B* **138**, 265 (1984);
J. Ellis, J.E. Kim and D.V. Nanopoulos, *Phys. Lett. B* **145**, 181 (1984).
- [34] M. Bolz, A. Brandenburg and W. Buchmüller, *Nucl. Phys.* **B606**, 518 (2001);
M. Bolz, A. Brandenburg and W. Buchmüller, *Nucl. Phys.* **B790**, 336 (2008) (E) [hep-ph/0012052];
J. Pradler and F.D. Steffen, *Phys. Rev. D* **75**, 023509 (2007) [hep-ph/0608344].
- [35] M. Kawasaki, K. Kohri and T. Moroi, *Phys. Lett. B* **625**, 7 (2005) [astro-ph/0402490];
M. Kawasaki, K. Kohri and T. Moroi, *Phys. Rev. D* **71**, 083502 (2005) [astro-ph/0408426];
R.H. Cyburt *et al.*, *Phys. Rev. D* **67**, 103521 (2003) [astro-ph/0211258];
J.R. Ellis, K.A. Olive and E. Vangioni, *Phys. Lett. B* **619**, 30 (2005) [astro-ph/0503023].
- [36] T. Schwetz, M. Tortola and J.W. F. Valle, *New. J. Phys.* **B13**, 063004 (2011) [arXiv:1103.0734];
T. Schwetz, M. Tortola, J.W.F. Valle, *New. J. Phys.* **B13**, 109401 (2011) [arXiv:1108.1376].
- [37] M.E. Gómez, G. Lazarides and C. Pallis, *Nucl. Phys.* **B638**, 165 (2002) [hep-ph/0203131];
G. Lazarides and C. Pallis, hep-ph/0406081;
N. Karagiannakis, G. Lazarides and C. Pallis, arXiv:1107.0667.
- [38] S. King and Q. Shafi, *Phys. Lett. B* **442**, 135 (1998) [hep-ph/9711288].
- [39] S.F. King and M. Oliveira, *Phys. Rev. D* **63**, 015010 (2001) [hep-ph/0008183].
- [40] I. Gogoladze, R. Khalid, S. Raza and Q. Shafi, *J. High Energy Phys.* **055**, 12 (2010) [arXiv:1008.2765];
I. Gogoladze, R. Khalid and Q. Shafi, *Phys. Rev. D* **80**, 095016 (2009);
I. Gogoladze, R. Khalid and Q. Shafi, *Phys. Rev. D* **79**, 115004 (2009) [arXiv:0903.5204].
- [41] K. Dimopoulos *et al.*, *J. High Energy Phys.* **05**, 057 (2003) [hep-ph/0303154].
- [42] See, e.g. T. Moroi, hep-ph/9503210; J. Pradler, arXiv:0708.2786; A. Ferrantelli, arXiv:1002.2835.
- [43] K. Maeda, *Phys. Rev. D* **39**, 3159 (1989);
D.I. Kaiser, *Phys. Rev. D* **81**, 084044 (2010) [arXiv:1003.1159].
- [44] S.R. Coleman and E.J. Weinberg, *Phys. Rev. D* **7**, 1888 (1973).
- [45] D.H. Lyth and A. Riotto, *Phys. Rept.* **314**, 1 (1999) [hep-ph/9807278];
A. Mazumdar and J. Rocher, *Phys. Rept.* **497**, 85 (2011) [arXiv:1001.0993].
- [46] G. Lazarides, *J. Phys. Conf. Ser.* **53**, 528 (2006) [hep-ph/0607032];
D. Baumann, arXiv:0907.5424.
- [47] D.S. Salopek, J.R. Bond and J.M. Bardeen, *Phys. Rev. D* **40**, 1753 (1989);
F. Bauer and D.A. Demir, *Phys. Lett. B* **665**, 222 (2008) [arXiv:0803.2664];
N. Makino and M. Sasaki, *Prog. Theor. Phys.* **86**, 103 (1991);
R. Fakir, S. Habib and W. Unruh, *Astrophys. J.* **394**, 396 (1992);
D.I. Kaiser, *Phys. Rev. D* **52**, 4295 (1995) [astro-ph/9408044]
T. Chiba and M. Yamaguchi, *J. Cosmol. Astropart. Phys.* **10**, 021 (2008) [arXiv:0807.4965].
- [48] C.P. Burgess, H.M. Lee and M. Trott, *J. High Energy Phys.* **09**, 103 (2009) [arXiv:0902.4465];
J.L.F. Barbon and J.R. Espinosa, *Phys. Rev. D* **79**, 081302 (2009) [arXiv:0903.0355];
C.P. Burgess, H.M. Lee and M. Trott, *J. High Energy Phys.* **07**, 007 (2010) [arXiv:1002.2730];
R.N. Lerner and J. McDonald, *J. Cosmol. Astropart. Phys.* **04**, 015 (2010) [arXiv:0912.5463];
M.P. Hertzberg, *J. High Energy Phys.* **11**, 023 (2010) [arXiv:1002.2995];
F. Bezrukov *et al.*, *J. High Energy Phys.* **016**, 01 (2011) [arXiv:1008.5157];
M. Atkins and X. Calmet, *Phys. Lett. B* **697**, 37 (2011) [arXiv:1011.4179].
- [49] A.D. Linde, *Phys. Lett. B* **129**, 177 (1983);
V.N. Şenoğuz and Q. Shafi, *Phys. Lett. B* **668**, 6 (2008) [arXiv:0806.2798];
E. Ramirez and D.J. Schwarz, *Phys. Rev. D* **80**, 023525 (2009) [arXiv:0903.3543].
- [50] S. Mooij and M. Postma, *J. Cosmol. Astropart. Phys.* **09**, 006 (2011) [arXiv:1104.4897].
- [51] L. Kofman, A.D. Linde and A.A. Starobinsky, *Phys. Rev. Lett.* **73**, 3195 (1994) [hep-th/9405187];
L. Kofman, A.D. Linde and A.A. Starobinsky, *Phys. Rev. D* **56**, 3258 (1997) [hep-ph/9704452].

- [52] J. Garcia-Bellido, D. G. Figueroa and J. Rubio, *Phys. Rev. D* **79**, 063531 (2009) [arXiv:0812.4624];
F. Bezrukov, D. Gorbunov and M. Shaposhnikov, *J. Cosmol. Astropart. Phys.* **06**, 029 (2009) [arXiv:0812.3622].
- [53] G.N. Felder, L. Kofman and A.D. Linde, *Phys. Rev. D* **59**, 123523 (1999) [hep-ph/9812289].
- [54] M. Endo, M. Kawasaki, F. Takahashi and T.T. Yanagida, *Phys. Lett. B* **642**, 518 (2006) [hep-ph/0607170];
M. Endo, F. Takahashi and T. T. Yanagida, *Phys. Rev. D* **76**, 083509 (2007) [arXiv:0706.0986].
- [55] C. Pallis, *Nucl. Phys.* **B751**, 129 (2006) [hep-ph/0510234].
- [56] V.N. Senoguz, *Phys. Rev. D* **76**, 013005 (2007) [arXiv:0704.3048].
- [57] K. Abe *et al.* [T2K collaboration], arXiv:1106.2822;
G.L. Fogli *et al.*, *Phys. Rev. Lett.* **101**, 141801 (2008) [arXiv:0806.2649].
- [58] G.L. Fogli *et al.*, *Phys. Rev. D* **66**, 093008 (2002) [hep-ph/0208026].
- [59] M. Apollonio *et al.*, *Phys. Lett. B* **466**, 415 (1999) [hep-ex/9907037].
- [60] S. Antusch, J. Kersten, M. Lindner and M. Ratz, *Nucl. Phys.* **B674**, 401 (2003) [hep-ph/0305273].
- [61] M. Fukugita and T. Yanagida, *Phys. Rev. D* **42**, 1285 (1990).
- [62] S. Davidson and A. Ibarra, *Phys. Lett. B* **535**, 25 (2002) [hep-ph/0202239];
T. Hambye, Y. Lin, A. Notari, M. Papucci and A. Strumia, *Nucl. Phys.* **B695**, 169 (2004) [hep-ph/0312203].
- [63] N. Arkani-Hamed and S. Dimopoulos *J. High Energy Phys.* **06**, 073 (2005) [hep-th/0405159];
G.F. Giudice and A. Romanino, *Nucl. Phys.* **B699**, 65 (2004) [hep-ph/0406088].
- [64] L. Randall and R. Sundrum, *Nucl. Phys.* **B557**, 79 (1999) [hep-th/9810155];
G. Giudice, M. Luty, H. Murayama and R. Rattazzi, *J. High Energy Phys.* **12**, 027 (1998) [hep-th/9810442].
- [65] R. Jeannerot and M. Postma, *J. Cosmol. Astropart. Phys.* **12**, 006 (2005) [hep-ph/0507162].
- [66] M. Arai, S. Kawai and N. Okada, arXiv:1107.4767.